Maternal Adaptations and Lipid Mobilization During Pregnancy in Rats

by

Dani Chalil

A thesis

presented to the University of Waterloo

in fulfillment of the

thesis requirement for the degree of

Master of Science

in

Kinesiology

Waterloo, Ontario, Canada, 2017

AUTHOR'S DECLARATION

I hereby declare that I am the sole author of this thesis. This is a true copy of the thesis, including any required final revisions, as accepted by my examiners.

I understand that my thesis may be made electronically available to the public.

Abstract

Docosahexaenoic acid (DHA) is a major structural fatty acid in brain and is required for fetal growth and development. DHA in maternal plasma increases during pregnancy to meet the placental transport demands of the fetus. Previously, we observed that 16:0/DHA phosphatidylcholine (PC) increased dramatically in plasma during pregnancy which was associated with increased hepatic expression and activity of phosphatidylethanolamine N-methyltransferase (PEMT), an enzyme that produces PC. Using hepatic tissue from the same rodent model, various pathways involved in lipid synthesis and secretion that could also support maternal DHA mobilization were presently examined. Targeted mRNA expression and immunoblotting assessments were used. In addition, a quadrupole-time of flight tandem mass spectrometry lipidomic method using alternating low-energy full-scan MS scans and high-energy collision-induced dissociation MS/MS scans (QTOF-MS^E) was used to examine changes across various acyl species of lipids at baseline, 15 days and 20 days of pregnancy, and 7 days postnatal. There was an increased mRNA expression of both ApoA1 and ApoA2, consistent with previous data. However, it appears this was not a result of increased expression of lipoprotein assembly enzymes examined. Surprisingly, there was no evidence of an upregulation of an acyltransferase, but PLA2G15, a phospholipase, was decreased throughout pregnancy in both mRNA and immunoblot analysis. This could be evidence of reduced phospholipid remodeling, considering the previous observation of the upregulation of PEMT. Lipidomic analyses revealed widespread changes in numerous acyl species of lipids in plasma and liver across all pregnancy time-points although comprehensive acyl species identification was not possible due to the nature of MS^E data. Nevertheless, there was evidence of depleted hepatic DHA levels at the postnatal time point. We have gained further insight into lipid synthesis and mobilization throughout pregnancy, and into novel lipidomic techniques.

Additional research is needed to determine the lipid species identify of numerous detected compounds in the present analysis. In addition, the decreased DHA status of several hepatic lipid species, indicates that future studies examining the post-partum period and the effect of lactation is warranted.

Acknowledgments

I would like to first thank my supervisor Dr. Ken Stark. You've given me an amazing opportunity and I'm thankful for it every day. I'm thankful for all the time you've given me to discuss all my ideas and I'm excited to see what the next four years have in store. I'll always owe you for making me a better scientist and more importantly a better person.

I'd like to thank my committee Dr. Robin Duncan and Dr. Russ Tupling for their support and guidance throughout this project. Thank you to everyone in the Stark lab, Jan, Adrian, and Tasha, with especial thanks to Juan, who helped make this project possible. You've taught me everything I know in this lab, and without your constant help, I'd be forever lost. You're the best role model I can hope for and I'm proud to call you a friend. Thank you to Ryan from the Duncan lab, Emma and Cat from the Tupling lab and everyone in the Physiology floor for your constant help and support.

Finally, special thanks go to my friends and family, Alan, my parents and of course Stella. I wouldn't be where I am without you and your constant love and support.

Table of Content

List of Tables

List of Figures

List of Abbreviations

ABCA1 – ATP-binding cassette transporter, sub-family A1
Acsl – Acyl-CoA synthestase
AGAPT – 1-acyl-glycerol-3-phosphate acyltransferase
ApoA – Apolipoprotein A
ApoB – Apolipoprotein B
ARA – Arachidonate
BCA – Bicinchoninic acid
CE – Cholysteryl ester
CEPT – choline/ethanolamine phosphotransferase
CPT – Choline phosphotransferase
CoA – Coenzyme A
DAG – Diacylglycerol
DDA- Data dependent aquisition
DHA – Docosahexaenoic acid
DNA – Deoxyribonucleic acid
DPA – Docosapentaenoic acid
FID – Flame ionization detector
G3P – Glycerol 3 phosphate (G3P)
GC – Gas chromatography
GPAT – Glycerol-3-phosphate acyltransferase
HDL – High density lipoprotein
IDL – Intermediate density lipoprotein
IMM – Inner mitochondrial membrane
LCPUFA – Long chain polyunsaturated fatty acids
LDL – Low density lipoprotein
LPCAT – Lysophophatidylcholine acyltransferase
LPEAT – Lysophosphatidylethanolamine acyltransferase
MS – Mass spectrometry
MTTP – Microsomal triglyceride transfer protein
PA – Phosphatidic acid
PC – Phosphatidylcholine
PCA – Principal component analysis
PE – Phosphatidylethanolamine
PI – Phosphatidylinositol
PLA_1 – Phospholipase A_1
PLA_2 – Phospholipase A_2
PUFA – Polyunsaturated fatty acids
PS – Phosphatidylserine
PEMT – Phosphatidylethanolamine N-methyltransferase
PVDF – Polyvinylidene fluoride
RNA – Ribonucleic acid
RT-qPCR – Reverse transcriptase qualitative polymerase chain reaction
SM- Sphingomyelin
SREBP – Sterol response element binding protein
-*sn* – Stereospecific number
TAG – Triacylglycerol

UHPLC – Ultra high-performance liquid chromatography
VLDL – Very low-density lipoprotein

Chapter 1: Introduction

Docosahexaenoic acid (DHA) is an omega-3 fatty acid known for its integral role in fetal brain and neural development [1, 2]. Maternal DHA deficiency has been linked to cardiovascular dysfunction [3], decreased retinal electrophysiology [4], and spatial awareness [5] of the offspring. Several global populations consume low DHA level in their regular diets [6] with 90% of Canadian pregnant women consuming <200 mg/d of DHA [7]. Therefore, understanding maternal DHA requirements is a public health concern. However, maternal plasma DHA levels increase during pregnancy by 5-7 folds suggesting a metabolic adaptation to meet fetal demand [8]. The underlining mechanism behind this adaptation is not fully understood. Reports of gene expression assessments of enzymes involved in fatty acyl specific lipid metabolism and lipidomic profiling to identify changes in acyl specific complex lipids of maternal tissues during pregnancy are very limited in the literature. Using these approaches with a pregnant rat model could help unravel pathways involved in lipid mobilization and synthesis during pregnancy.

Previously, using a rodent pregnancy model, we confirmed that maternal plasma DHA increased, and then attributed most of the increase to a change in palmitoyl-docosahexaenoyl-phosphatidylcholine (16:0/DHA-PC) (Chalil et al, 2017, *submitted*). The increase in 16:0/DHA-PC was associated with an increase in the expression and activity of phosphatidylethanolamine N-methyltransferase (PEMT) as well as an increased expression of FADS2. This coordinates well with a previous observation that PC synthesized by PEMT is selectively transferred by the placenta to the fetus [9]. There is also evidence that PEMT selectively converts DHA-containing phosphatidylethanolamine to PC, but that normally, the DHA content of this new PC is rapidly lowered through acyl chain remodeling [10]. In this study, we examine the mRNA expression of enzymes involved in lipid synthesis including acyltransferases, phospholipases as well as lipoprotein assembly enzymes to further understand the mechanism surround DHA mobilization. Based on the mRNA expression results, immunoblotting was then used to determine protein levels of enzymes of interest. A comprehensive lipidomic analysis of plasma and liver samples was also performed using UHPLC-MS/MS analyses with a QTOF-MS/MS (Waters Synapt G2Si mass spectrometer, Waters

Limited, Mississauga, ON) using alternating low/high energy scans. This untargeted approach provided MS/MS data for all compounds (better known as MS^E) which allowed us to establish a profile of the most abundant lipid species, and assess lipid profile changes during pregnancy and post-partum.

Chapter 2: Biochemical Foundations

Understanding DHA and its role in fetal development requires an in-depth knowledge of phospholipids, their synthesis, and remodeling through the Lands' cycle. As various metabolic pathways are involved in the synthesis and secretion of lipids, knowledge of key structural changes in acyl specific lipids can shed light on what enzymes are responsible for these transformations. Similarly, the transport of these lipids and fatty acyls to the placenta is largely via lipoproteins, therefore lipoprotein assembly should also be examined.

While pregnancy is associated with increased plasma total lipids, and there is considerable data on fatty acid profiles during pregnancy, there is little data on fatty acyl species of complex lipids across various maternal tissues. Some data on maternal plasma lipidomic profiles during pregnancy has been reported [11], but non-pregnant baseline values were not determined and a metabolic perspective including the role of hepatic lipid synthesis and mobilization was not considered. A more comprehensive examination of lipidomic changes is needed to potentially identify mechanisms leading to hyperlipidemia in pregnancy and selective transport of acyl-specific lipids through lipoproteins.

2.1 Importance of DHA during pregnancy

DHA has both structural and functional roles in the brain and retina as the brain matter is 60% fat of which 35-40% are polyunsaturated fatty acids (PUFA) [12]. DHA makes up 40-50% of brain PUFA and it is distributed in membranes of synapses, the cerebral cortex, mitochondria and photoreceptors in the retina [2]. DHA is also important for decreasing phospholipid bilayer viscosity, and DHA incorporation leads to more efficient signal transduction [13]. In addition, DHA metabolites such as N-docosahexaenoylethanolamide appear to mediate synaptogenesis and hippocampal neuronal growth [14]. In rat models, a deficient supply of DHA during pregnancy and rearing causes impaired learning and spatial awareness in offspring [5, 15]. Maternal plasma DHA levels increase during pregnancy in what appears to be a metabolic adaptation to meet fetal demand during the third trimester [16] in order to support the brain growth spurt [17]. This increase in maternal DHA is largely in the PC pool, and more specifically 16:0/DHA-PC and is associated with

PEMT expression and activity (Chalil et al, 2017 *submitted*). Evidence also points to selective placental uptake of PC synthesized by PEMT [9], which is believed provide PC enriched with DHA as compared with PC from the Cytidine Diphosphocholine (CDP-choline pathway) [18]. Once synthesized, these PC molecules are then incorporated into VLDL for plasma transport to the placenta. This points to the to the importance of understanding phospholipid synthesis as they appear to be important carriers of DHA during pregnancy

2.2 De novo phospholipid synthesis

Phospholipids can be synthesized by different pathways which may have a role in DHA mobilization during pregnancy and postpartum [9, 19]. "Phospholipids" (PL) is a broad term typically applied to membrane lipids that contain a phosphate moiety in the head group. Glycerophospholipids tend to dominate cell membrane composition and are characterized by a glycerol backbone with a polar head group in the stereospecific number (*sn*)-3 position. Sphingolipids are another type of PL, but contain a sphingoid base backbone rather than a glycerol backbone. The most abundant subclasses of PL are phosphatidylethanolamines (PE), phosphatidylcholines (PC), phosphatidylinositols (PI), phosphatidylserines (PS), and sphingomyelins (SM). PC is the dominant PL eukaryotic in membranes followed by PE with the other types being considerably lower in the plasma membrane bilayer of eukaryotes. Additionally, PC is largely found in the outer membrane layer and PE in the inner membrane layer [20]. This is due to a larger head group for PC as the choline group in PC is larger and fills the outer curvature of membranes, while the smaller ethanolamine group in PE is required for the inner curvature. There is also a tendency for PE to have a higher PUFA content resulting in outward "splayed" acyl chains, while PC tends to have a more compact acyl chain profile associated with higher saturated and monounsaturated content.

PL synthesis is a multi-organelle process spanning the cytosol, endoplasmic reticulum, and the inner mitochondrial membrane (IMM) [21]. This synthesis is first initiated with the transfer of an acyl group from an acyl-CoA to a glycerol 3 phosphate (G3P) catalyzed by glycerol-3-phosphate

acyltransferases (GPAT). GPAT, which encompasses 4 different isomers, are found in both the IMM as well as the ER [21]. GPAT 1 and 2, which are the isomers found in the IMM, appear to have high specificity for saturated acyl CoAs, while GPAT 3 and 4 are found in the cytosol and do not have this specificity. GPATs produce 1-acyl-Glycerol-3-phopshate, or lyso-phosphatidic acid (LPA) that are further acylated by 1-acyl-glycerol-3-phosphate acyltransferases (AGPAT), forming phosphatidic acid (PA). In the committed step for the synthesis of both PE and PC, PA is converted into a diacylglycerol (DAG) by lipid phosphate phosphohydrolases.

The synthesis of PC can occur through multiple pathways, with the primary being the Kennedy pathway in hepatic tissue (**Figure 1**) [22]. The CDP-choline pathway originates with choline kinase that phosphorylates choline to P-choline. The phosphorylated choline is converted to CDP-choline by CTP-phosphocholine cytidylyltransferase and then PC is formed by either choline phosphotransferase (CPT) or choline/ethanolamine phosphotransferase (CEPT). Hepatic tissue is also capable of synthesizing PC through the methylation of PE pathway that accounts for ~30% of PC in hepatocytes [18, 23]. This PE methylation pathway, unlike the Kennedy pathway, does not require choline obtained through dietary means and relies only on PEMT to convert PE to phosphatidylmonomethylethanolamine, phosphatidyldimethylethanolamine, and finally PC [24].

PE comprises 20-40% of phospholipids in mammalian bilayers, and is synthesized through two main pathways. The main pathway of PE synthesis in hepatic tissues is the CDP-ethanolamine pathway [25], which is similar to the CDP-choline pathway (**Figure 1**). Interestingly, ethanolamine phosphotransferase which transfers the ethanolamine head-group to a DAG also preferentially selective for substrates (DAG) containing DHA in the *sn*-2 position [26]. This selectivity highlights another enzyme integrated into the mechanism of DHA mobilization in pregnancy. PE can also be synthesized in the PS decarboxylation pathway [27] in the inner mitochondrial membrane by PS decarboxylase.

2.3 Phospholipid acyl chain remodeling

PL in eukaryotes have distinct fatty acid distributions. Saturated and monounsaturated fatty acids are predominantly esterified in the *sn*-1 position, while polyunsaturated fatty acids, are predominantly esterified in the *sn*-2 position. PL can undergo remodeling of these fatty acids by a series of acylation/de-acylation reactions with the help of acyltransferases and phospholipases that make up Lands' cycle (**Figure 2**) [28, 29]. After the de-acylation by a phospholipase, an "activated" fatty acid that is bound to coenzyme A (CoA) can be acylated back into the PL by an acyltransferase. This family of enzymes contain isoforms specific for different types of PL, *sn*-positions for acyl placement and specific to affinities for different fatty acids. The expression of acyltransferase isoforms is also largely dependent on the tissue type, and they can be influenced by physiological state. For example, lyso-PC acyltransferase 4 (LPCAT4) is highly expressed in the epididymis with specificity for 18:1 while lyso-PE acyltransferase 1 (LPEAT1) is highly expressed in the brain with specificity for 18:0. GPAT 1-4, AGPAT 1-4, and LPCAT 1-4 are possible acyltransferases that regulate DHA remodeling during pregnancy through PA synthesis.

Similarly, there are isoforms of phospholipases with different specificities. Phospholipase A1 targets acyl groups in the *sn*-1 position while phospholipase A2 targets acyl groups in the *sn*-2 position. The "activation" of the fatty acids is highly similar, as the Acyl-CoA synthetase can be fatty acid specific and dependent on its saturation level. Acsl 3/6 are two isomers that have been shown to possess a strong affinity for DHA making them possible targets to explain increased DHA incorporation into PL during pregnancy [30, 31]. The phospholipase A_2 superfamily, which hydrolyzes fatty acids in the *sn*-2 position of phospholipids, has been categorized into 6 distinct types that cumulatively include 16 different groups. Each of these groups differs based on their mechanism of action, structure, interaction with membranes, and biological activities. A number of these groups (Groups 4a, 5, 6, 10, 15, and 16) have been identified to act on certain PC species turning them into lyso-PC for further remodeling through Lands' cycle [32-37].

2.4 Hepatic Lipoprotein Assembly

Plasma lipoproteins are mainly found in 4 types (VLDL, LDL, IDL, and HDL) that differ based on their protein density. These particles are made up of a monolayer of PC, cholesterol, and proteins that surround nonpolar lipids such as triacylglycerols (TAG) and cholesteryl esters (CE) [38]. The proteins found in these vesicles, referred to as apolipoproteins, assist phospholipids in surrounding and transferring lipids, while also serving as enzyme cofactors, and receptor ligands.

The incorporation of DHA into lipoproteins in postprandial state is well documented. Labelled DHA infusion in tracer studies shows over 85% incorporation into TAG of VLDL and LDL within 30 minutes [39]. This incorporation of DHA into VLDL particles appears to be selective when compared to palmitate and EPA [40]. DHA has also been shown to incorporate into the inner core of HDL particles [41], however the mechanism surrounding DHA incorporation is not well understood. Examining enzymes involved in lipoprotein assembly might provide insight into mobilization of hepatic DHA into plasma and placenta thereafter to meet fetal demand.

The dominant apolipoprotein class is Apolipoprotein B (ApoB) and is associated with chylomicrons, VLDL and LDL particles. There are two ApoB isoforms based on the origin of synthesis in either the small intestine (ApoB 48) or the liver (ApoB 100) [42]. Prior to hepatic VLDL release, VLDL assembly is initiated by the synthesis of ApoB in the ER followed by its glycosylation [43]. The ER also acts as a site of glycerolipid synthesis which occupies the lipid core of the lipoprotein, and is transferred into the precursor VLDL by the microsomal triglyceride transfer protein (MTTP) [44-46]. The lipid center also contains CE which potentially links the rate of VLDL assembly to cholesterol biosynthesis through HMG-CoA reductase [47]. While HMG-CoA reductase is considered the rate-limiting enzyme in cholesterol biosynthesis, it is regulated by the presence of mature Sterol Response Element Binding Protein (SREBP), a transcription factor that also induces the expression of VLDL production and other lipogenic enzymes [48]. Increased expression of MTTP or SREBP could indicate that increased hepatic production and secretion of VLDL is occuring.

HDL differs from VLDL and LDL by the presence of apolipoprotein A (ApoA) and its

assembly pathway. ATP-binding cassette transporter, sub-family A1 (ABCA1) is a membrane protein responsible for the production of HDL particles [49]. By catalyzing the efflux of both PL and free cholesterol to ApoA1, it allows the formation of heterogeneous sized HDL particles. The size of these particles are solely dependent on its activity [50].

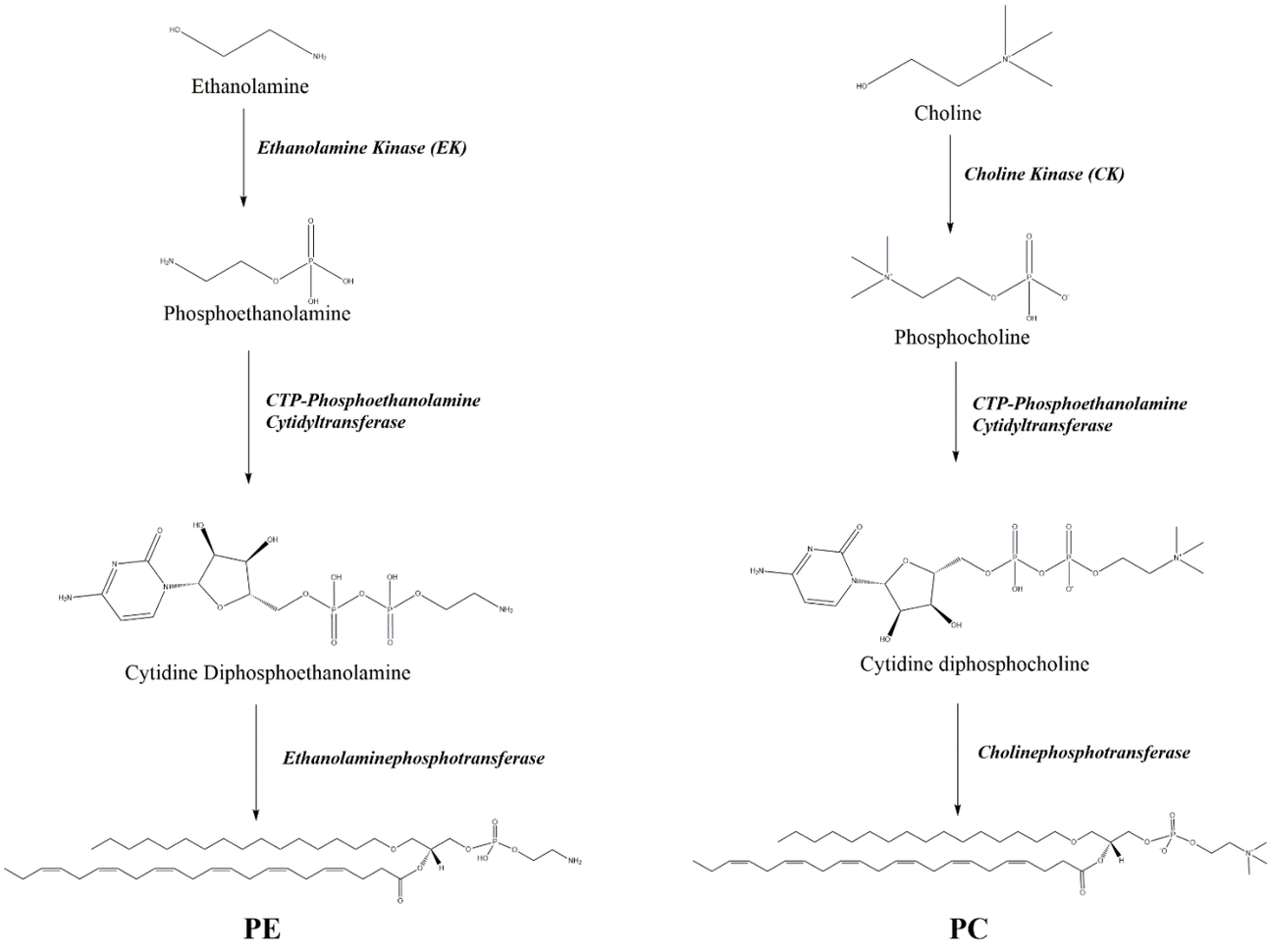

Figure 1: The Kennedy pathway for PE and PC synthesis (adapted from Gibellini and Smith, 2010) [51]

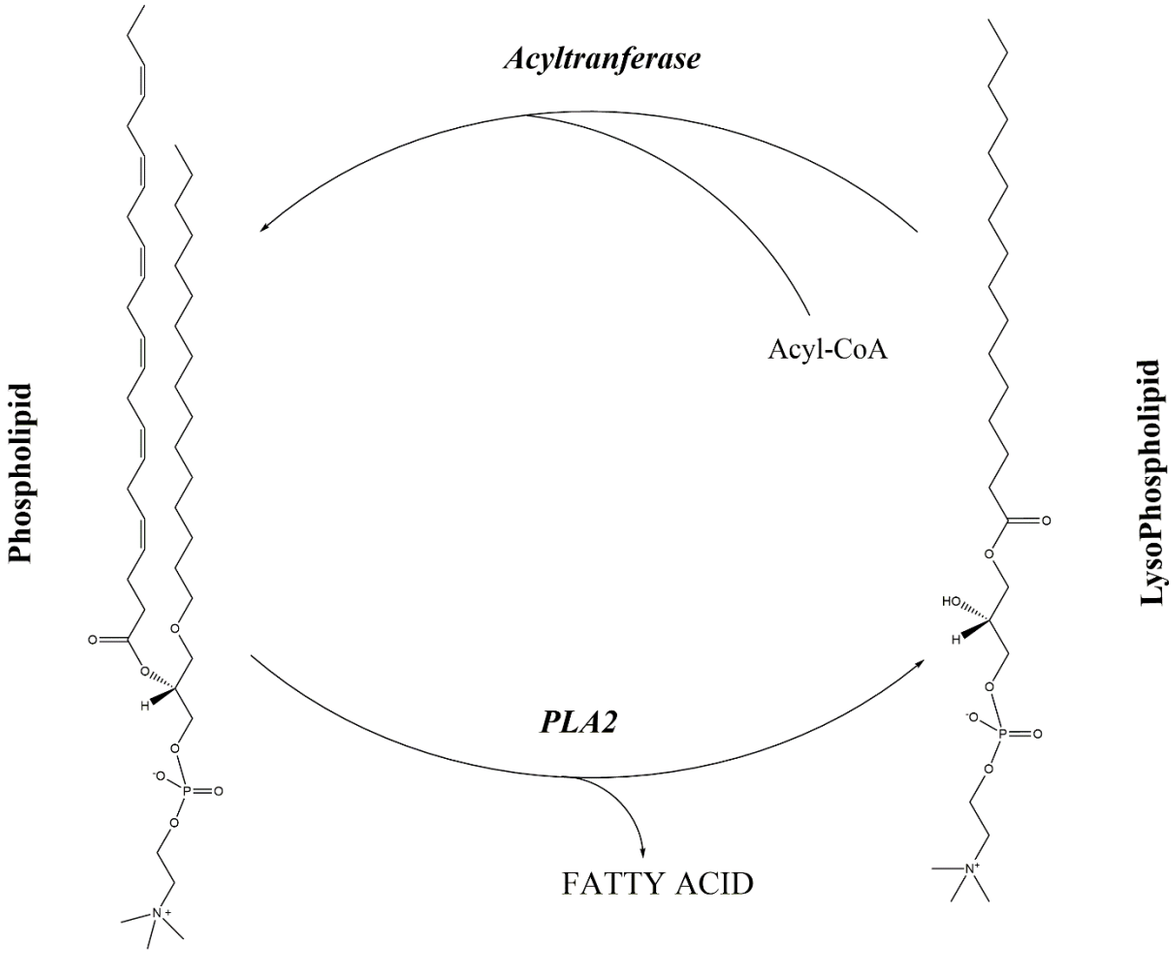

Figure 2: Lands' Cycle (adapted from Shimizu 2009)[52]

Chapter 3: Rational, hypotheses, and objectives

3.1 Rationale

Docosahexaenoic acid (DHA) is required for proper neurodevelopment during pregnancy [17]. There appears to be various physiological adaptations to ensure adequate delivery of DHA to the fetus. While much of this research has focused on adaptations by the placenta itself [53, 54], maternal adaptions to supply DHA to the placenta are less studied. Understanding these maternal metabolic adaptations involved with maternal-fetal transport of DHA are important to establish dietary recommendations for DHA for women during pregnancy. Currently, the Institute of Medicine does not have such a recommendation, but rather a recommendation of 1.4g/d of 18:3n-3 for women during pregnancy [55]. Health Canada recommends 150g/week of fish during pregnancy as a source of EPA and DHA, but do not indicate a specific quantity of DHA to consume [56]. A recommendation of 200 mg/d of DHA for pregnant women has been made by an expert panel [57], but the possibility of increased biosynthesis of DHA and mobilization of DHA was not considered in this evaluation of the literature.

Previous work from our lab has shown that increased 16:0/DHA phosphatidylcholine is associated with increased expression and activity of PEMT and increased expression of FADS2. Increased expression of FADS2 could result in a higher biosynthesis of DHA from 18:3n-3 and partially explain increased DHA concentrations, but does not explain the very specific increase in 16:0/DHA PC as the DHA produced from FADS2 would be in the form of an Acyl-CoA. Interestingly, PC synthesized from PEMT appears to be selectively transferred to the fetus [9] In addition, PEMT has been shown to have selectivity for DHA containing PE substrates, but the resulting PC usually undergoes rapid acyl chain remodeling to lower DHA content and have a fatty acyl profile similar to the existing PC pool [10]. Examinations of PL synthesis and remodeling enzymes during pregnancy are very limited, but acyl chain specificities in PL metabolism could have a considerable role in making DHA available for secretion into plasma as a lipoprotein component.

The prior observation of increased 16:0/DHA PC in plasma suggests that DHA transport to the fetus from the liver is as part of the PC monolayer of lipoproteins. While hyperlipidemia during pregnancy is well documented [58], the exact mechanism is not well defined. Examining lipoprotein assembly enzymes during pregnancy could provide additional insight into the increase in 16:0/DHA PC in plasma.

Lastly, the previous observation of increased 16:0/DHA PC during pregnancy was the result of a constrained semi-targeted lipidomic analytical approach. Only day 15 and day 20 of pregnancy were examined (selected based on DHA changes in the fatty acid composition data) and only plasma PC and liver PC and PE pools were examined. Plasma lipidomic profiles of pregnant women have been reported [11] but without any comparison with before or after pregnancy, so it is difficult to determine specific adaptations during pregnancy. Lipidomic assessments of all lipid classes from baseline through pregnancy to post-partum in plasma and liver could provide further insights into adaptations of maternal lipid metabolism during pregnancy and provide potential enzymes and pathways to target for further examination.

3.2 Objectives

This thesis has two main objectives with both contributing to our understanding of maternal adaptations in fatty acid and lipid synthesis and mobilization during pregnancy. Both objectives will use tissues collected from chow fed Sprague Dawley rats in a pregnancy protocol that included baseline, day 15 of pregnancy, day 20 and 7 days post-partum time points.

The first objective was to examine the gene expression of various PL synthesis and remodeling enzymes and of lipoprotein assembly proteins in liver. Initially, mRNA expression was to be examined, and then based on these findings, targeted determinations of protein concentrations were completed with available antibodies.

The second objective was to complete comprehensive, untargeted lipidomic analyses on both plasma and liver samples throughout pregnancy. To complete this objective, UHPLC-MS/MS analyses were completed on a QTOF-MS/MS instrument at the University of Waterloo Mass

Spectrometry Facility that uses an alternating low/high energy scans to generate MS and MS/MS spectra of compounds. This "MS^E" data was then to be processed using Progenesis software package (Nonlinear Dynamics, Newcastle, UK) to: 1) determine the most abundant acyl-specific lipid species in these tissues and 2) use principal component analysis to determine individual lipids that change the most throughout pregnancy and post-partum.

3.3 Hypotheses

1. There will be an increased expression of LPCAT1 in maternal hepatic tissue relative to baseline to accommodate the incorporation of DHA into lyso-PC.
2. There will be an increased expression of Acsl 3, to accommodate the increased DHA remodeling through acyltransferases.
3. There will be a decrease in the expression of PLA2G15 in maternal hepatic tissue relative to baseline to reduce the remodeling of PC newly synthesized by PEMT.
4. There will be an increased expression of MTTP, ABCA1, as well as SREBP at the end of pregnancy compared to baseline to support increased VLDL assembly.
5. Plasma 16:0/DHA-PC at baseline and postpartum will be similar, and lower than levels at day 20.
6. Hepatic 16:0/DHA-PC at baseline and postpartum will be similar, and lower than levels at day 20.

Chapter 4: Gene and protein expression

4.1 Introduction

The increased presence of plasma DHA during pregnancy has been extensively studied, due to its key role in fetal development. More recent data have linked this to an increase in DHA in the PC pool. PC appears to have preferential uptake by the placenta [9]. Previous work from our lab show an increase in the PEMT pathway through mRNA, protein, and activity assay assessments, throughout pregnancy [19]. This is could be an adaptive mechanism for the increased production of DHA enriched PC. An examination of PEMT in primary hepatocytes cultured from non-pregnant female rats indicated PEMT selectively converted DHA containing PE to PC but the new PC was rapid remodeled to remove DHA so that the final DHA content of the PEMT synthesized PC resembled the preexisting pools of PC in the hepatocytes [10]. In previous work, we observed that increased 16:0/DHA PC was associated with increased PEMT expression and activity, suggesting some form of adaptation in phospholipid acyl chain remodeling during pregnancy. This post synthesis remodeling of PC would limit the ability to export DHA as a component of lipoproteins during pregnancy. To determine the enzymes responsible for this remodeling adaptation, liver samples from a previous study were analyzed using the RT-qPCR and Western blotting technique.

4.2 Design

All animal procedures were approved by the University of Waterloo Animal Care Committee and are in accordance with the guidelines of the Canadian Council on Animal Care. The samples that were analyzed were collected in a previous study (as described in Chalil, 2013 [19]).

Briefly, twenty-four female Sprague Dawley rats were purchased at 7 weeks of age. A baseline group of non-pregnant rats (n=6) were sacrificed after 7 days of acclimatization while others were mated with 6-month old proven male breeders (Envigo, Mississauga, ON Canada) at the Central Animal Facility on campus. All rats were fed a commercial fixed formula rodent diet (8640 Teklad 22/5 Rodent Diet, Envigo) providing 3.0 kcal/g with 17% of energy from fat, 29%

energy from protein and 54% energy from carbohydrate throughout the study. Pregnant rats (n=6) were sacrificed at day 15 and day 20 of pregnancy, and 7 days postnatal. All sacrifices were by exsanguination following anesthesia, using isoflurane, after an overnight fast. Exsanguinated blood was collected in the presence of EDTA and plasma was isolated by centrifugation at 1500g and the liver was excised, washed in saline (0.9% v/v), and weighed. Samples were flash frozen in liquid nitrogen and stored at -80°C for various analyses.

4.3 Methods

4.3.1 Gene Expression

mRNA expression was determined by reverse transcriptase qualitative polymerase chain reaction (RT-qPCR), a technique used to amplify and detect a specific sequence of RNA. RNA extraction was performed using Trizol reagent containing RNAse inhibitor. Separation of RNA from other cellular component was done using chloroform. After centrifuging the RNA into a pellet, it was washed with ethanol and dissolved in water. RNA purity was measured using a NanoDrop spectrophotometer, and samples with high purity (260/280 ratio above 1.80) were used for subsequent cDNA synthesis by reverse transcriptase. Following extraction from the samples, the sequences were reverse transcribed to cDNA for higher stability on a thermo-cycler. The samples cDNA, of similar concentrations, were loaded on a plate alongside the forward and reverse primers for the intended gene with the addition of SYBR Green. The primers were designed through the Primer-BLAST program on the NCBI website and ordered from Sigma-Aldrich with the full list of primers and their sequences listed in **Table 1**. SYBR Green is a fluorescent dye that binds to double stranded DNA allowing detection of the product of qPCR. The samples were incubated at 95°C for 10 min, followed by 40 cycles of 95°C and 60°C in order to amplify the target sequence. The data was expressed relative to 18S which served as a house keeping gene during pregnancy [59].

4.3.2 Protein expression

Immunodetection was used to determine protein levels of the gene products as described previously [60]. Liver tissue was homogenized in a buffer (0.25mol/L sucrose, 0.01mol/L tris-HCl, 0.01mol/L $MgCl_2$, 2.5mmol/L DTT), containing complete protease and phosphatase inhibitors. Using a bicinchoninic acid (BCA) procedure, 40 µg of protein was resolved on a 15% SDS-PAGE gel and transferred to a polyvinylidene fluoride (PVDF) membrane. Subsequently, non-specific binding sites were blocked using 10% milk in TBS-T for 1 hour at room temperature. The membrane was then incubated with primary antibodies for PLA2G15 (Sigma-Aldrich, Saint Louis, Missouri using a 1:250 dilution) and β-actin (Sigma-Aldrich, Saint Louis, Missouri, using a 1:500 dilution) in a 5% milk TBS-T solution for 1 hour at room temperature. The membrane was further washed with TBS-T and incubated again for 1 hour at room temp with horseradish peroxidase-conjugated secondary antibody (goat anti-rabbit, Santa Cruz Biotechnology, 1:8000 dilution). Finally, the membrane was rewashed and using Enhanced Chemiluminescence Western Blotting Detection Reagents, the proteins were visualized on a Chemidoc instrument (BioRad, Mississauga, ON). Molecular weights of proteins, equal protein loading, and adequate transfer of protein to membrane were also confirmed by ponceau staining.

For statistical analyses, a one-way ANOVA test was used to determine differences in mRNA, protein, and lipids at the different time points of sample collection. All data is presented as means ± standard deviations. Statistical significance was determined at $P>0.05$ via a Tukey post hoc test after a significant *F* value was detected.

Table 1: List of target genes and SYBR green primers used to identify them.

Gene	Primer	Gene	Primer
Glycerol and acylglycerol phosphate acyltransferases		***Phospholipases***	
GPAT1*	Forward: 5′ ACCACATCAAGGATACAGCTCAT 3′ Reverse: 5′ GAATTGGGCAGATAAGAAACGTC 3′	PLA2G4a*	Forward: 5′ AGTCGGAACTGTGAAGGGC 3′ Reverse: 5′ TTCTTGAAGCAGTTCCCAGAGT 3′
GPAT3	Forward: 5′ GGAGGATGAAGTGACCCAGA 3′ Reverse: 5′ CCAGTTTTTGAGGCTGCTGT 3′	PLA2G5*	Forward: 5′ CTTGGGCTGCCAGCATAAAC 3′ Reverse: 5′ TTGGGTTCTTTTTAGCCTGGTCT 3′
GPAT4	Forward: 5′ AGCCCTACACCAACGGAATC 3′ Reverse: 5′ CTCTGGTGTCTTATCCAGAGCC 3′	PLA2G6*	Forward: 5′ GACTCTGAGCGTCCAGTCCT 3′ Reverse: 5′ TATGTGGGACAGGTAGGCGA 3′
AGPAT1*	Forward: 5′ CACAAAGAGACCACTAGGG 3′ Reverse: 5′ TTCCTCCCCATACCTGACAC 3′	PLA2G10	Forward: 5′ TGTCTCAGCGAAGCAACCAG 3′ Reverse: 5′ GTTCATGTAAGCCATCGGCG 3′
AGPAT2	Forward: 5′ AGCTCTTCACCTCAGGAACG 3′ Reverse: 5′ GGACTGGTAGCAAGTGTCCA 3′	PLA2G15	Forward: 5′ GTGCTGGTGCCTGGTGATTT 3′ Reverse: 5′ CCTCTTGGAGCACAGGTAGTG 3′
AGPAT4	Forward: 5′ GCCCAGCCTCAAGCATCA 3′ Reverse: 5′ ACATCTCGCAAGCACTTCACA 3′	PLA2G16*	Forward: 5′ CTAAACAAAGGCATCCACGGC 3′ Reverse: 5′ CTTGGGTTCTGGTATGGGCA 3′
Acyl-CoA synthetases		***Lysophosphatidylcholine acyltransferases***	
ACSL3	Forward: 5′ GGCTACTCTTCACCACAGACA 3′ Reverse: 5′ CGATCCATGATTTCCGGCAC 3′	LPCAT1	Forward: 5′ TGAGGGGCCTCGGACTAAAA 3′ Reverse: 5′ GCTGCAAACTCTGGAAGCCT 3′
ACSL6	Forward: 5′ TGAATGCACAGCTGGGTGTA 3′ Reverse: 5′ ATGTGGTTGCAGGGCAGAG 3′	LPCAT2	Forward: 5′ TTGTCGTTGCTCCTCACTCC 3′ Reverse: 5′ CCGTAACAGTCTGCCAACCA 3′
Apolipoproteins		LPCAT3	Forward: 5′ GCCTTAACAAGTTGGCGACG 3′ Reverse: 5′ AACGGGTAGCCCAGGAAGAT 3′
ApoA1	Forward: 5′ CAGGGTGAAGGATTTCGCCA 3′ Reverse: 5′ TCCAGGAGATTCAGGTTCAGC 3′	LPCAT4	Forward: 5′ GCCCTGGCGTACTCAAAGT 3′ Reverse: 5′ GCTGATAGACGGGGAGGAAC 3′
ApoA2	Forward: 5′ AGCCTAGAAGGAGCTTTGGT 3′ Reverse: 5′ TGGGCCTTCTCCATCAAATCC 3′	***Microsomal triglyceride transfer protein***	
ApoA4	Forward: 5′ GGCCAATGTGATGTGGGACT 3′ Reverse: 5′ CCTGGAAGAGGGTATTGAGCTG 3′	MTTP	Forward: 5′ AGGCTCCACTCAGGCAATTT 3′ Reverse: 5′ TTGATGGAGCGGGAGTTCAC 3′
ApoA5	Forward: 5′ CCAGGCTCGCTACTTTGTGA 3′ Reverse: 5′ TGCAAACACTGAGAGGAGGG 3′	***ATP-binding cassette transporter***	
ApoB	Forward: 5′ TGTCCAGCCCCATCACTTTAC 3′ Reverse: 5′ GGGGTGAGCCTTCTCAGTTT 3′	ABCA1	Forward: 5′ CGATTCATGGAGTGTGTCAACC 3′ Reverse: 5′ TCCTCGCATCCAATAGGTCC 3′
ApoE*	Forward: 5′ ATTCACCCAGGGGGCTTGA3′ Reverse: 5′ CAGGCATCCTGTCAGCAATGG 3′	***ADP ribosylation factor related protein***	
Sterol regulatory element-binding protein and phospholipid transfer proteins		ARFRP1*	Forward: 5′ GTCAAGGACCGTGAAGGGGT 3′ Reverse: 5′ TACATCCTGTTTGGCACCCTGT 3′
SREBF1	Forward: 5′ CCATGGACGAGCTACCCTTC 3′ Reverse: 5′ AGCATGTCTTCGATGTCGGT 3′	***Peroxisome proliferator-activated receptor***	
PLTP	Forward: 5′ TGAATGAGCGTATCTGGCGT 3′ Reverse: 5′ AACAGTGACGAAGCCTGCAT 3′	PPARα*	Forward: 5′ TCGGGGATCTTAGAGGCGA 3′ Reverse: 5′ ACAGAGCACCAATCTGTGATG 3′

* Primers which do not span the coding DNA sequence

4.4 Results

4.4.1 Acyltransferases

There was no clear increase of GPAT, AGPAT, or LPCAT mRNA expression throughout the four-time points (**Figure 3 and 4**). There was a significant decrease (maxed at 57%) in AGPAT2 mRNA at day 15 and 20 as compared with baseline ($P<0.05$), followed by a significant increase (218%) at 7 days postpartum compared to day 20 ($P<0.05$) (**Figure 3)**. Acsl 3 increased during pregnancy (day 15 and 20 compared to baseline) while Acsl 6 decreased (day 20 compared to baseline) ($P<0.05$). (**Figure 5**).

4.4.2 Phospholipases

There was a significant decrease in PLA_2G15 mRNA expression at end of the pregnancy (day 20 compared to baseline, 56%) ($P<0.05$), followed by a significant increase at 7 days postpartum compared to day 20 (401%) and baseline ($P<0.05$), suggesting PLA_2 downregulation during pregnancy (**Figure 6**). PLA_2 G5 and G16 displayed similar mRNA expression patterns to that observed with G15. However, this change was only significant in PLA_2 G16 ($P<0.05$), which had a 37.5% decrease at the end of pregnancy compared to postpartum followed by an increase to baseline levels postpartum (**Figure 6**).

Immunoblotting for PLA_2G15 resulted in protein level patterns that were similar to patterns observed with the mRNA results. Protein levels were decreased by 47% at the end of pregnancy (day 20) as compared with baseline ($P<0.05$). Expression increased in the postpartum as compared with day 20 by 34%, but remained below the original baseline levels ($P<0.05$).

4.4.3 Lipoprotein Assembly

ApoA1 mRNA increased significantly at day 15 and 20 of pregnancy compared with baseline (maxed at 337% increase) followed by a 65% decrease 7 day postpartum compared to day 20 ($P<0.05$) where it matched day 15 levels. ApoA2 mRNA expression had a gradual increase throughout pregnancy and into postpartum resulting in significant increase at day 20 and maxing at 175% higher expression at 7 days postpartum as compared with baseline (**Figure 9**) ($P<0.05$). There was no clear increase for any lipoprotein assembly proteins across pregnancy (**Figure 10)**. ARFRP1

mRNA was significantly decreased only at the end of pregnancy (day 20) as compared with baseline (37% decrease) ($P<0.05$), with a slight but non-significant increase in the postpartum (**Figure 10)**. PPARPα mRNA had no changes throughout pregnancy, but there was a significant increase in the postpartum (107 %) compared to day 20 ($P<0.05$) (**Figure 10)**. Finally, MTTP mRNA had a slow gradual increase throughout pregnancy which did not reach significance until 7 days postpartum as compared with baseline (93% increase) ($P<0.05$) (**Figure 10)**. All other mRNA proteins examined had no changes throughout pregnancy or postpartum (**Figure 10)**.

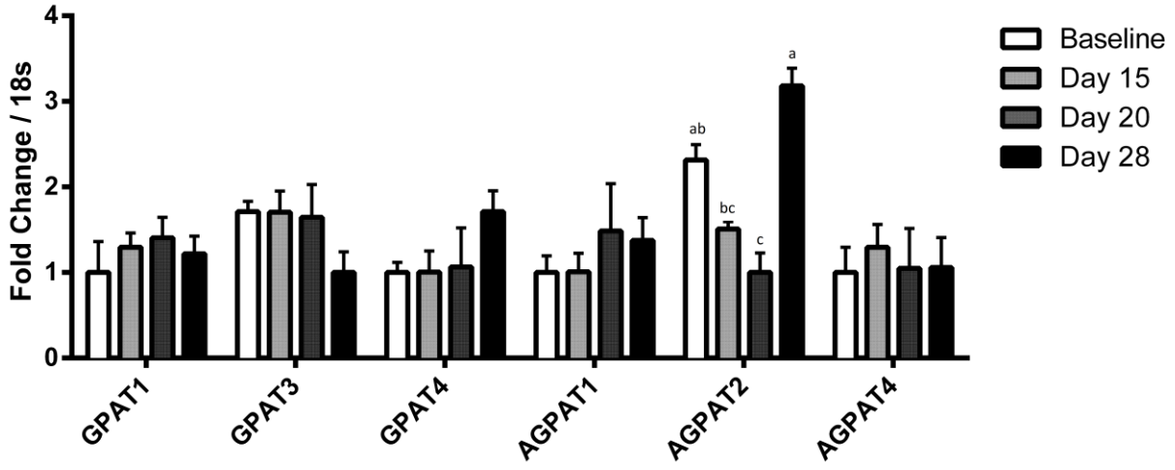

Figure 3: Pregnancy Effect on glycerol-3-phosphate acyltransferases (GPAT) and 1-acyl-glycerol-3-phosphate acyltransferases (AGPAT) mRNA expression in maternal liver. Values with different superscripts are significantly different. Values with no superscripts had no significance between the 4 groups. Significance is determined by Tukey's post hoc test ($p<0.05$) following significant F-value by one-way ANOVA.

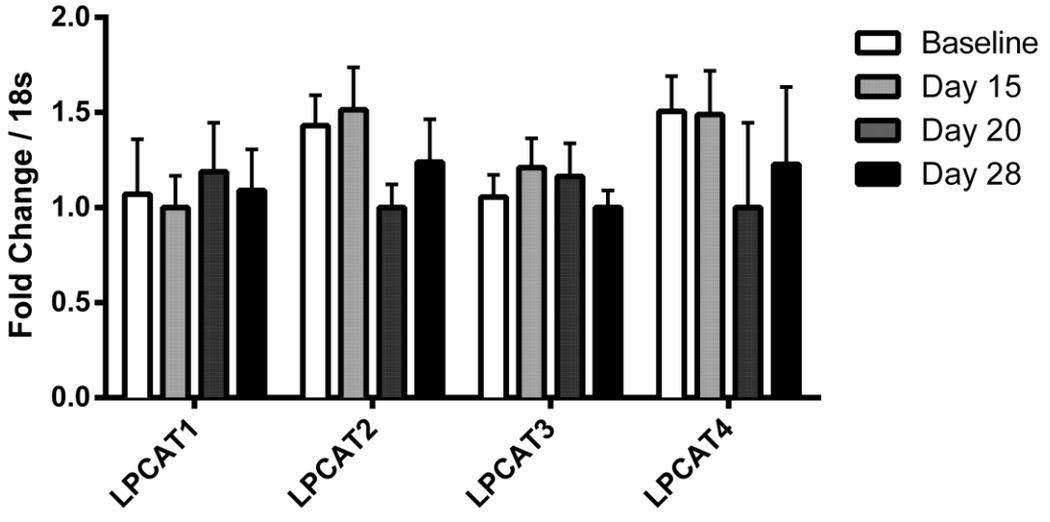

Figure 4: Pregnancy Effect on Lyso-phosphatidylcholine acyltransferases (LPCAT) mRNA expression in maternal liver. Values with different superscripts are significantly different. Values with no superscripts had no significance between the 4 groups. Significance is determined by Tukey's post hoc test ($p<0.05$) following significant F-value by one-way ANOVA.

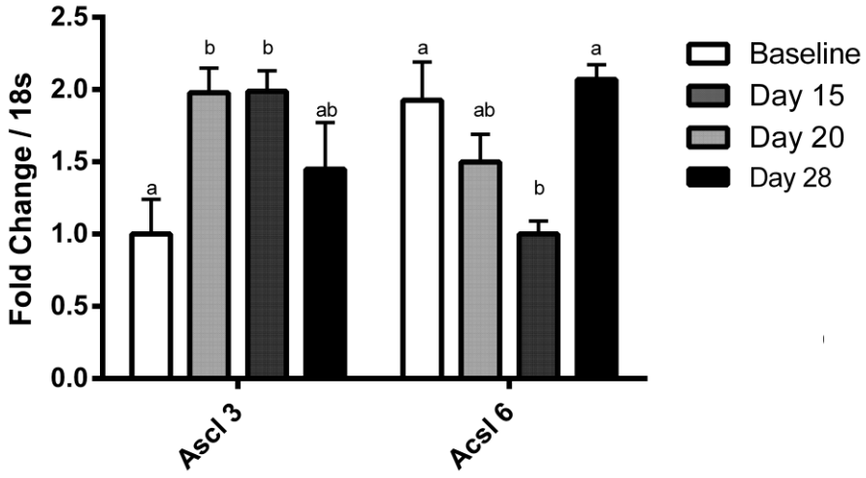

Figure 5: Pregnancy Effect on long-chain Acyl-CoA synthetases (Acsl) mRNA expression in maternal liver. Values with different superscripts are significantly different. Values with no superscripts had no significance between the 4 groups. Significance is determined by Tukey's post hoc test ($p<0.05$) following significant F-value by one-way ANOVA.

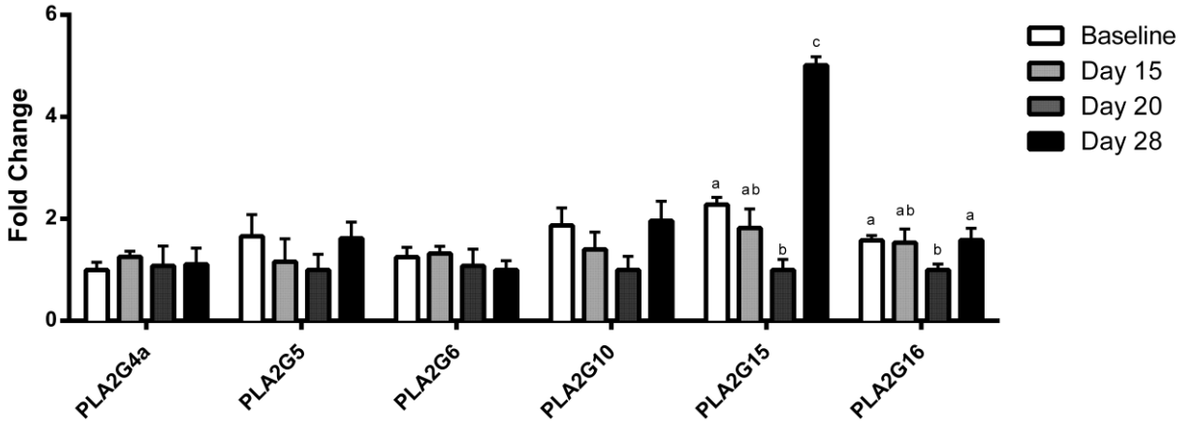

Figure 6: Pregnancy Effect on Phospholipase A_2 mRNA expression in maternal liver. Values with different superscripts are significantly different. Values with no superscripts had no significance between the 4 groups. Significance is determined by Tukey's post hoc test ($p<0.05$) following significant F-value by one-way ANOVA.

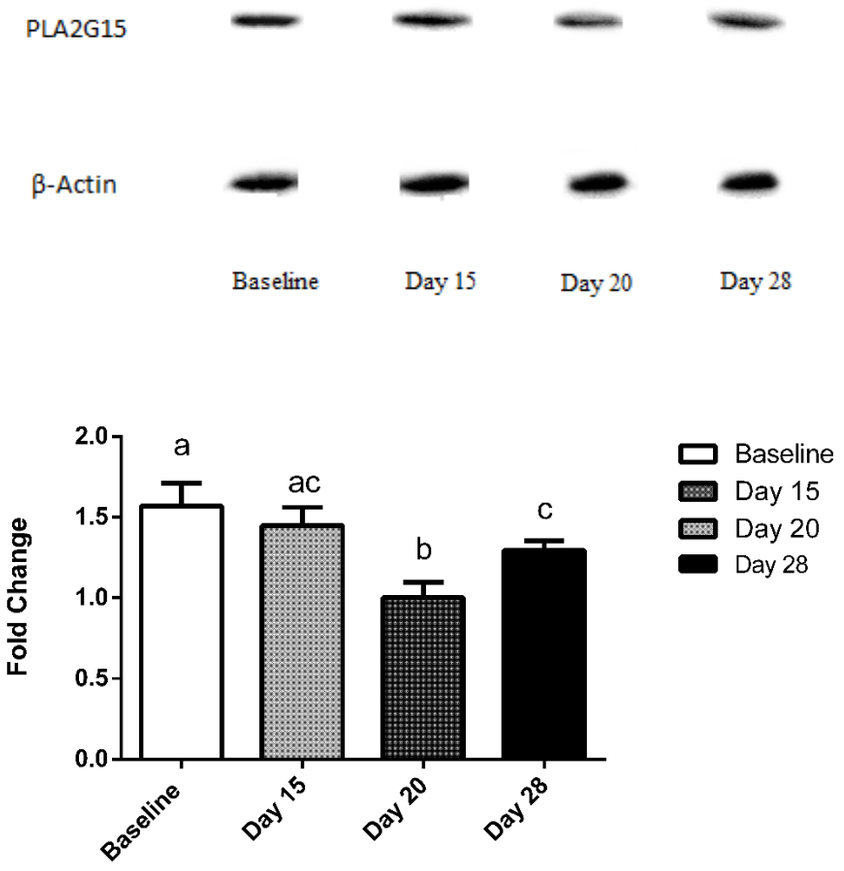

Figure 7: Pregnancy effect on PLA_2GXV protein expression in maternal liver. Significance is determined by Tukey's post hoc test ($p<0.05$) following significant F-value by one-way ANOVA.

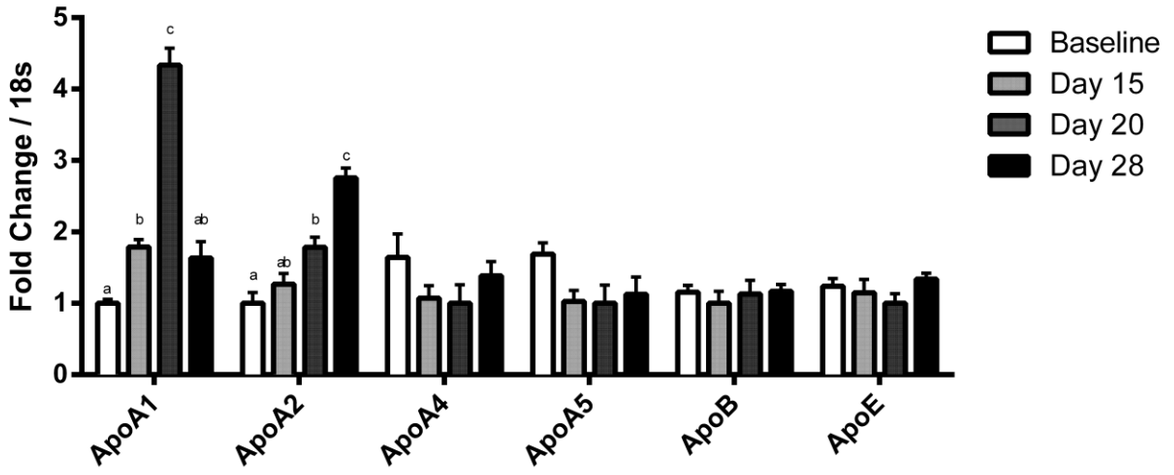

Figure 8: Pregnancy Effect on Apolipoprotein mRNA expression in maternal liver. Values with different superscripts are significantly different. Values with no superscripts had no significance between the 4 groups. Significance is determined by Tukey's post hoc test ($p<0.05$) following significant F-value by one-way ANOVA.

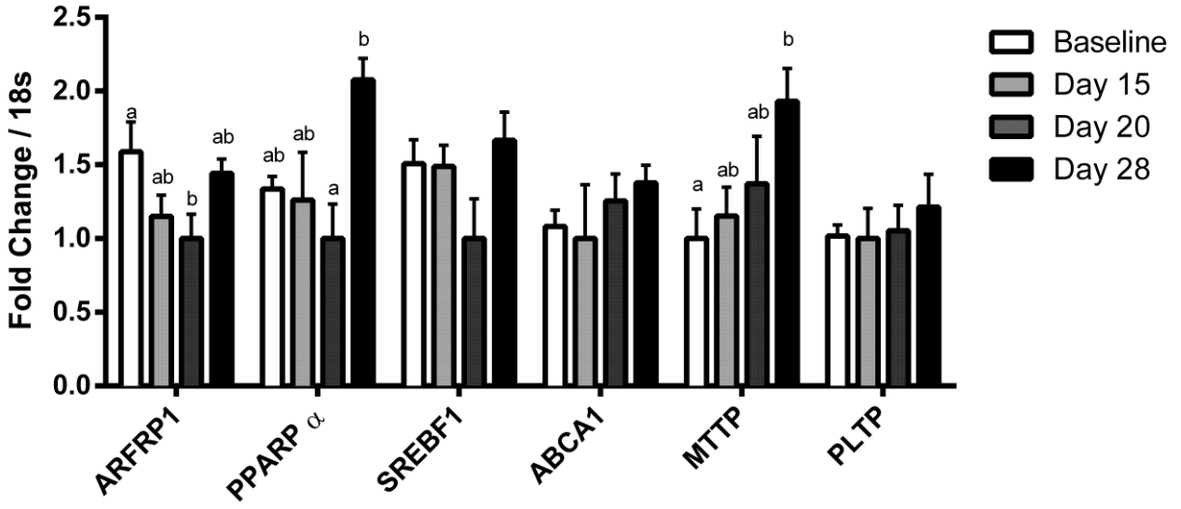

Figure 9: Pregnancy Effect on Lipoprotein assembly proteins mRNA expression in maternal liver. Values with different superscripts are significantly different. Values with no superscripts had no significance between the 4 groups. Significance is determined by Tukey's post hoc test ($p<0.05$) following significant F-value by one-way ANOVA.

4.5 Discussion

The mRNA levels of AGPAT 2, Acsl 6, PLA2G15 and PLA2G16 all decreased during pregnancy, suggesting decreased remodeling of phospholipids during pregnancy. As each of these enzymes participates in a part of the remodeling cycle, the decreased overall expression should allow DHA enriched PC levels to remain elevated in the liver for export to the plasma. AGPAT2 specific action in converting LPA to PA is possibly downregulated in pregnancy to limit the synthesis of saturated phospholipids such as PE. This in turn yields higher relative abundance of unsaturated acyl chains in PE for conversion to PC. Similarly, the downregulation of Acsl 6 is thought to limit post synthesis remodeling of PC to assist in maintaining high abundance of DHA containing PC. Due to a limitation of available antibodies, we were limited to testing PLA2G15 protein levels. PLA2G15, did decrease throughout pregnancy, providing further support of downregulation of acyl chain remodeling during pregnancy. PLA2G16 decreased mRNA levels during pregnancy suggest that decreased acyl chain remodeling of PC, lyso-PC and PE, as this enzyme has been shown to possess phospholipase A1 and A2 activity, and in vivo acyltransferase activity [61, 62]. Similar to previously available data, the increased levels of ApoA1 and A2 mRNA levels during pregnancy indicates increased lipoprotein production as a mechanism for pregnancy induced hyperlipidemia [63]. This occurs despite decreased levels of both ARFRP1 and PPARP α mRNA levels, and no changes in other lipoprotein assembly mRNA that we examined. Changes in activity rate could be another possible mechanism causing increased lipoprotein production and hyperlipidemia during pregnancy.

Interestingly, there is a clear increase in the remodeling enzymes mRNA levels in the postpartum period. Theoretically, this would result in decreased levels of DHA-enriched PC, but previous data does show plasma DHA remains elevated as compared with baseline levels [19]. Adaptations to mobilize maternal DHA may remain during the postpartum to provide the offspring DHA through maternal breastmilk. Mammary tissue is capable of synthesizing DHA enriched PC through mechanisms similar to the liver. Further examination of gene expression in mammary tissue in the postpartum is necessary to evaluate this mechanism of action and understand DHA offspring transport during this period. This will, however, require validation in humans as the postpartum

phenomena observed presently may be specific to rodents due to a later brain growth spurt that occurs across pregnancy and the postpartum [64].

Chapter 5: Lipidomic Analyses

5.1 Introduction

The increase of blood lipids through pregnancy is well documented, where total cholesterol, LDL, HDL, and TAG can increase as much as four-fold [58]. Examining the fatty acid composition of each complex lipid fraction is possible through the use of thin layer chromatography combined with gas chromatography. However, this approach only provides the fatty acid composition of an entire lipid class and individual acyl species cannot be identified. Tandem mass-spectrometry can provide this information but it has yet to be applied to the study of pregnancy-induced hyperlipidemia. We have identified one report of plasma lipidomic analyses in pregnant women [11], but mechanistic insights are not possible as baseline data was not collected and dietary assessment was not completed. Using a rat model allows us to control collection time points and diet. In addition, we are able to examine liver tissue, the main site of lipogenesis. To determine the most abundant lipid species in both plasma and liver during pregnancy, samples from the same previous study [19] were analyzed using a Waters Quadrupole-Time of Flight (QTOF) mass spectrometer to generate MS/MS data across all compounds (MS^E). This data was also used in comparison with previously acquired data in which only day 15 and 20 time-points were examined.

5.2 Design

All animal procedures were approved by the University of Waterloo Animal Care Committee and are in accordance with the guidelines of the Canadian Council on Animal Care. The samples that were analyzed were collected in a previous study (as described in Chalil, 2013 [19]). Briefly, twenty-four female Sprague Dawley rats were purchased at 7 weeks of age. Rats sacrificed at baseline, 15 and 20 days of pregnancy and 7 days postpartum and tissues were collected as described in section 4.2

5.3 Methods

5.3.1 Non-targeted lipidomic analyses

Lipids were extracted from 50uL plasma or 50mg frozen pulverized liver tissue using a modified Folch procedure [65] with 3mL 2:1:0.5 chloroform:methanol:0.2M NaH_2PO_4 buffer. Lipid extracts were diluted in chloroform by a factor of 10 to prevent signal saturation in the mass spectrometer. Samples were spiked with an internal standard mix containing a mixture of different classes of deuterated lipids at relevant physiological concentrations (Splash Lipidomix, Avanti Polar Lipids, Alabaster, AL). Lipid extracts were dried under a stream of N_2, and then resuspended in 100uL 65:35:5 isopropanol:acetonitrile:water +0.1% formic acid. A reversed-phase, binary multi-step UHPLC protocol was used with a C18 Acquity CSH column with dimensions 150mm x 2.1mm x 1.7 μm (Waters Limited, Mississauga, ON) for plasma samples, and a C18 Ascentis Express column with dimensions 150mm x 2.1mm x 2.0μm (Sigma-Aldrich, St. Louis, MO) for liver samples. The mobile phase consisted of A: 60:40 acetonitrile:water +10mM ammonium formate +0.1% formic acid with pH = 4.3, and B: 90:10 isopropanol:water +10mM ammonium formate +0.1% formic acid with pH = 5.8. The gradient protocol used was as follows: 0 – 1.5 minutes it was 32% B, from 1.5 – 4 min 45% B, from 4 – 8 min 50% B, from 8 – 18 min 55% B, from 18 – 20 min 60% B, from 20 – 35 min 70% B, from 35 – 40 min 95% B, from 40 – 45 min 95% B, from 45 – 47 min B was decreased to 32%, and allowed to equilibrate until the 48-minute mark. The flow was set to 260μL/min, column temperature at 45°C, and tray temperature at 4°C. A Waters Synapt G2Si Quadrupole-Time of Flight (QTOF) mass spectrometer (Waters Limited, Mississauga, ON) was used in positive electrospray ionization mode. The instrument was set to MS^E resolution mode, with a scan range of 100-1200 and a spray voltage of +2kV. The Waters MassLynx software (version 4.1, Waters Limited, Mississauga, ON) was used for extracting ion chromatograms, integrating peak areas, and generating MS/MS spectra.

Data was imported into Progenesis QI (v2.3, Nonlinear Dynamics, Newcastle, UK) for principal component analysis (PCA) to detect differences across groups and for preliminary compound identification. Progenesis import settings were set to default filters with $[M+H]^+$ and $[M+NH_4]^+$

adducts, and the peak filter set to 2. PCA processing uses the low energy, full-scan MS data, which can be used to determine the total number of carbons and double bonds in a molecule but cannot distinguish between specific acyl species in a complex lipid. This can be used to generate a lipid's "*Brutto*" species [66]. MS/MS data is required to identify specific acyl chains within a lipid (sometimes called "*Medio*" species) and when possible, ratios of different MS/MS fragments can allow determinations of acyl chain -*sn* positioning ("*Genio*" species). Identifications were acquired using the ChemSpider search engine using KEGG, LipidMAPS, MassBank, ChemBank, ChEBI and ChEMBL databases with a 5ppm precursor tolerance and use both MS and MS/MS data. EZinfo v3.0.3.0 was used to generate s-plots between two time-points using orthogonal projections to latent structures discriminant analysis (OPLS-DA) models to identify significantly different compounds between two time-points.

PCA retains most of the relevant information from the original dataset but remaps the data in a reduced space defined by principal components to explain the variation[67]. Mathematically, PCA defines each point using the equation:

$$\mathbf{D} = \mathbf{T}\,\mathbf{P}^{\mathbf{T}} + \mathbf{E}$$

D is the data matrix, **T** is the score matrix and $\mathbf{P}^{\mathbf{T}}$ is the loading matrix and **E** is the matrix of residual error. These values are obtained by means of maximum explained variance and orthogonality. Score and loading matrices are produced during the analysis that contain the coordinates of the samples in space of principal component as well as the importance of each of the original variables in describing the principal components respectively. The PCA graphs in this thesis are representations of scores and loadings in the space defined by component 1 and component 2, which is considered the most common graphic representation due to it having the highest explained variance score.

5.4 Results

5.4.1 Selective analysis

Several PC and PE species were examined throughout all the time points (**Figure 11 and 12**). During pregnancy, there was a significant increase in PC plasma levels of 32:0, 32:1, 34:2, 36:4, 38:6 (16:0/DHA), and 40:6 (18:0/DHA) (P>0.05) (**Figure 11**). PC 32:1, 34:1 and 36:1 both increased significantly in the postpartum, while 38:6, and 40:6 both decreased during this time point (P>0.05) (**Figure 11**). Liver PC had subtle but significant changes where 32:0, 32:1, 36:1, 36:2, and 38:4 all decreased at the end of pregnancy compared with baseline (P>0.05) (**Figure 12**). 34:0-PC, 40:6-PC (18:0/DHA) and more clearly 38:6-PC (16:0/DHA) all increased at the end of pregnancy as compared with baseline (P>0.05). 32:0-PC, 32:1-PC. 36:4-PC, 38:6-PC (16:0/DHA), and 40:6-PC (18:0/DHA) all decreased in the postpartum (P>0.05) (**Figure 12**). 34:2-PE, 36:2-PE, 36:4-PE, 38:4-PE, and 40:7-PE all decreased with pregnancy (P>0.05), however only 34:2-PE, 36:2-PE, and 38:4-PE increased again in the postpartum (P>0.05) (**Figure 12**).

5.4.2 Highest abundance

The top 85% most abundant lipids in both plasma and liver in baseline rats were first determined to establish a referencing point for other time point analyses. The 85% highest abundant lipid species in baseline plasma (**Table 2 and Table S1**) included 802 compounds. Identifications were attempted for the top 50% (90 compounds) of which only 33 were positively identified. The lipids identified were predominately phosphatidylcholines, in which 38:4-PC, 36:2-PC, 34:4-PC, 34:2-PC, 38:6-PC and 40:6-PC made up 11% of total abundance. Other lipids such as lyso-PC, and TAG were also present but contributed to less than 1% each to the total abundance.

The 85% most abundant lipid species in the liver (**Table 3**) included 158 compounds with 57 positive identifications. The lipids were mostly PC and TAG in which 10 compounds making up over 43% of total abundance with 38:4-PC (18:0/20:4n-6) making up almost 12% of total abundance of lipids in the liver.

5.4.3 PCA and S-plots

The principal component analysis graphs for plasma and liver can be found in **Figure 13**. Plasma PC1 and PC2 had explained variance of 29.7% and 16.8% respectively. Liver PC1 and PC2 had 44.1% and 17.0% respectively. The clustering of each time point (denoted with different colors) is indicative of differences being present. The s-plots of each time point for both plasma and liver can be found in **Figure 14 and 15** respectively. These s-plots were used to detect significant changes between two time-points. Significant compounds can be detected in the top right and bottom left quadrants. Most changes are observed when examining baseline vs. day 20 and 28, as well as day 20 vs. day 28.

Plasma differences between baseline and day 15 (**Table 4**) show several TAG and DAG species increasing with 20:5 - cholesteryl ester (CE) decreasing. At day 20 of pregnancy, hyperlipidemia is quite clear when compared to baseline (**Table 5**), as we see 60:9 TAG increase 66 and 32 fold for the two isomers detected. PE and PC species also increased. Most notable was 38:6-PE with a 55-fold increase and 38:4-PC with a 32-fold increase. The increase in 38:6-PE (most likely 16:0/DHA-PE, but not confirmed) is however minimal when compared with 16:0/DHA-PC as the PC species had a maximal abundance 59 times higher than that of the PE species.

When compared with baseline, day 28 plasma samples have changes in several unidentified compounds and/or specialized lipids (**Table 6**). A number of PC and TAG species were elevated at day 28 upwards of 8-fold, while 20:5-CE decreased compared with baseline. Fold changes in the plasma lipidome at day 15 vs. day 20 of pregnancy (**Table 7**), day 15 of pregnancy vs. 7 days postpartum (**Table 8**) and day 20 of pregnancy vs. 7 days postpartum (**Table 9**) reiterates that hyperlipidemia occurs during pregnancy with increases in both PE and PC, TAG species and many unidentified lipids during pregnancy time points.

Liver differences identified between baseline and day 15 of pregnancy (**Table 10)** show different TAG species increasing at day 15 of pregnancy, most notable of which was TAG 57:2 with a 3.94-fold increase. Comparison between baseline and day 20 of pregnancy (**Table 11**) shows PC, lyso-PC, PE and TAG differences in which only two species (16:0/DHA-PC and 40:5-PE) increased

with pregnancy. There was also an increase in 16:0/DHA-PC at day 20 of pregnancy. The comparison of baseline to day 28 of pregnancy (**Table 12**) provides a pattern shared among all significant lipid species, which is a decrease in the post-partum. Interestingly many of the changes are were unidentified. Differences between hepatic day 15 and 20 of pregnancy, highlighted in **Table 13**, show 40:5-PE, 16:0/DHA-PC, 48:5-PC, 50:2 TAG, and 40:8-PC increasing in day 20. In the post-partum, 40:5-PC and 40:5-PE continued to increase **(Table 14)**, as highlighted in liver differences between day 15 and 28 of pregnancy. There was also a notable decline in 60:12 TAG which decreased 3.6 folds in the postpartum. Finally, **Table 15** presents a 5.37-fold decrease in 16:0/DHA-PC in the postpartum compared to the end of pregnancy (day 20). Similarly, there was a decrease in 58:8 TAG, 56:5-TAG, 56:6 TAG, 40:5-PC, 56:8 TAG, 56:7 TAG, and 48:5-PC. Interestingly, 36:2-PE was the only compound to increase in this comparison window.

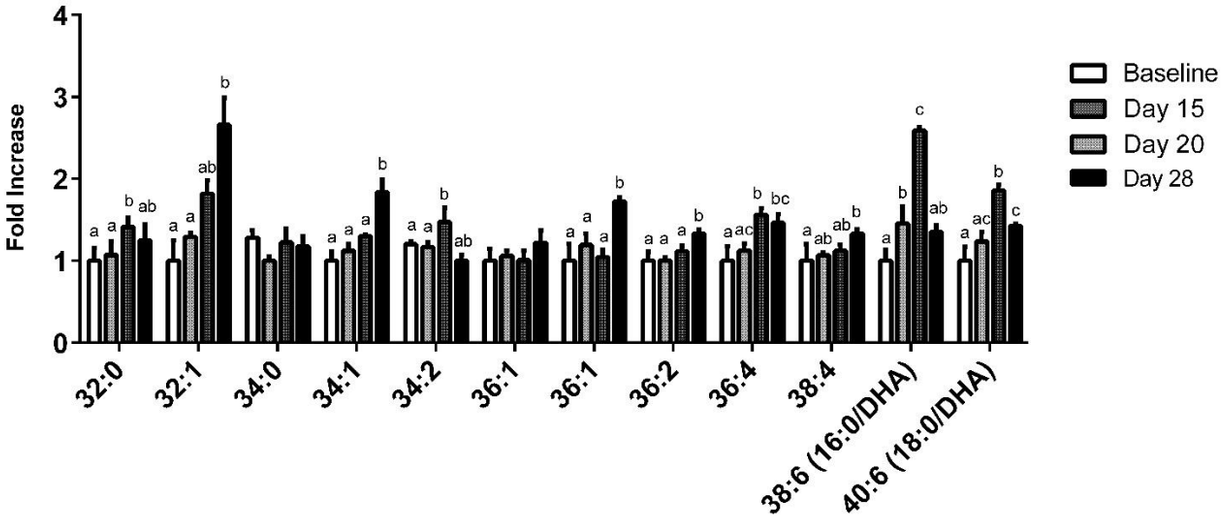

Figure 11: Changes in plasma phosphatidylcholine species across the four different time points of pregnancy. Bars with different superscripts significantly different across time within a specific lipid. Significance was determined by Tukey's post hoc test ($p<0.05$) following a significant F-value by one-way ANOVA.

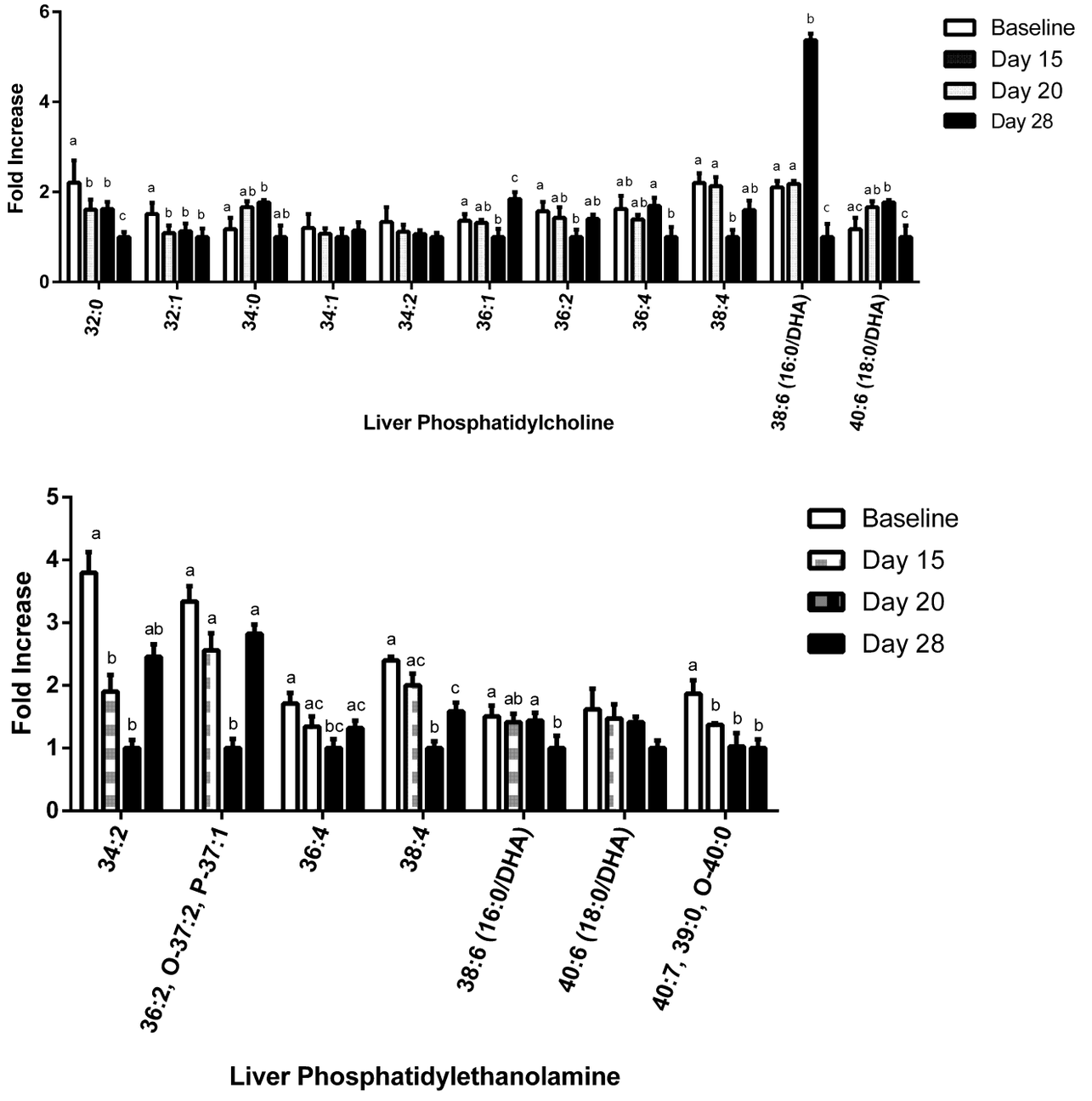

Figure 12. Changes in liver phosphatidylcholine (A.) and phosphatidylethanolamine (B.) species across the four different time points of pregnancy. Bars with different superscripts were significantly different across time within a specific lipid. Significance was determined by Tukey's post hoc test ($p<0.05$) following a significant F-value by one-way ANOVA. Acronyms: O-, indicates alkyl ether; P-, indicates alkenyl ether; DHA, docosahexaenoic acid;

Table 2. List of top 85% most abundant compounds in plasma samples of nonpregnant female rats (n=4)

M/z	Retention Time	Identification	Abundance	Cumulative Abundance %
810.6095	16.96	38:4-PC	828030	2.34
786.6087	17.60	36:2-PC	781729	4.54
754.6257	14.93	34:4-PC	718112	6.57
758.5778	14.10	34:2-PC	645050	8.39
806.5777	12.71	38:6-PC (16:0/DHA)	584241	10.03
834.6079	15.89	40:6-PC	567368	11.64
829.8066	29.99		517183	13.09
782.5772	13.54	36:4-PC	497760	14.50
524.3818	4.60		464964	15.81
1128.3188	26.97		435349	17.04
738.6544	13.51		431913	18.26
496.3490	3.54	16:0 lyso-PC	419808	19.44
1054.2992	26.14		413553	20.61
758.2235	21.47		396971	21.73
980.2799	25.20		363177	22.75
872.7762	29.30	52:4 TAG	336545	23.70
832.2421	22.97		336041	24.65
1047.7415	4.59		334686	25.59
906.2606	24.16		324301	26.51
874.7924	30.15	52:3 TAG	312940	27.39
760.5919	16.82	34:1-PC	301731	28.24
570.5543	12.76	Cer(d18:0/h17:0)	300530	29.09
529.4077	3.63		292673	29.92
803.5468	5.81		261050	30.65
520.3467	3.06	18:0 lyso-PC	237100	31.32
815.7056	24.08		232918	31.98
991.6787	3.52		228315	32.62
369.3593	29.85		228102	33.27
896.7762	28.96		215794	33.87
808.5893	13.61	38:5-PC	212312	34.47
544.3472	2.97	20:4 lyso-PC	209786	35.07
369.3590	31.50		207697	35.65
690.6230	29.84		197924	36.21
944.7732	27.69		195308	36.76
788.6222	20.54	36:1 PC	194532	37.31
813.6906	22.37		182190	37.82
703.5795	13.23	PE-Cer(37:1)	176004	38.32
675.6836	31.42		168504	38.80
522.3612	3.65	18:1 lyso-PC	163804	39.26
784.5888	14.30	36:3-PC	162719	39.72
894.7570	28.18		161027	40.17
1027.0005	31.41		160805	40.62

M/z	Retention Time	Identification	Abundance	Cumulative Abundance %
369.3573	30.44		156912	41.07
900.8057	30.15		147340	41.48
920.7722	28.05		146924	41.90
898.7899	29.28		145773	42.31
876.8086	30.94		138728	42.70
550.6296	19.94		137975	43.09
637.3108	3.75		136839	43.48
836.6190	16.99	40:5-PC	132473	43.85
787.6727	22.49	GlcCer (d16:1/23:0)	130314	44.22
922.7910	28.93		128447	44.58
1024.7361	3.52		127475	44.94
942.7557	26.87		123972	45.29
570.5542	29.99	Cer(d18:0/h17:0)	123390	45.64
666.6227	30.44		120747	45.98
898.7920	29.81		120223	46.32
627.5399	13.82		119948	46.65
415.2171	1.86		119798	46.99
565.5735	21.62		119707	47.33
946.7896	28.61		113904	47.65
924.8056	29.78		113483	47.97
811.6707	20.71	SM (d18:2/24:1)	112056	48.29
801.6880	23.31		109025	48.60
1069.7190	4.61		104885	48.89
593.6046	23.41		104280	49.19
537.5396	18.39		103861	49.48
695.5780	29.87		102605	49.77
887.5669	13.82	38:4-PI	101119	50.05
762.6038	20.27	34:0-PC	98349	50.33
877.7267	29.28		97785	50.61
949.7263	27.69		96946	50.88
812.6182	18.53	38:3-PC	95966	51.15
782.5720	12.00		95692	51.42
920.7750	28.52	56:8 TAG	95003	51.69
834.7549	29.94	49:2 TAG	90631	51.94
965.6997	27.69		89043	52.20
893.7006	29.31		86799	52.44
848.7727	30.15	TAG 50:2	86448	52.68
813.6864	22.70	GlcCer (d18:2/23:0)	85172	52.92
742.5625	12.77		81047	53.15
917.7005	28.96		80122	53.38
901.7272	28.95		79809	53.60
671.5770	30.44		77522	53.82

Table 3. List of top 85% most abundant compounds in liver samples of nonpregnant female rats (n=4)

Compound mass (m/z)	Identification	Retention time	Abundance	Cumulative Abundance %
810.60130	38:4- PC (18:0/20:4n-6)	18.25	8245235	11.92
872.77043	52:4 TAG	30.35	3984831	17.69
874.78835	52:3 TAG	31.25	3839177	23.24
782.56953	36:4-PC (16:0/20:4n-6)	14.06	2993945	27.57
758.56969	34:2-PC	15.07	2168399	30.70
786.59981	36:2-PC	19.75	1958702	33.54
898.78392	54:5 TAG	30.32	1874840	36.25
876.80407	52:2 TAG	32.11	1717149	38.73
806.56947	38:6-PC (16:0/DHA)	13.25	1658626	41.13
900.80226	54:4 TAG	31.20	1339587	43.07
829.79925		31.15	1060320	44.60
768.55460	38:4 PE	18.26	855622	45.84
893.69962		30.37	819973	47.02
764.52327	38:6-PE	13.24	807597	48.19
760.58461	34:1-PC	18.27	777677	49.31
429.24085		5.37	765697	50.42
803.54403		5.30	747469	51.50
895.71552		31.28	696578	52.51
902.81733	54:3 TAG	32.05	679478	53.49
808.58369	38:5-PC	14.40	639774	54.42
848.77080		31.32	600044	55.29
920.76709	56:8 TAG	29.53	555325	56.09
832.58177	40:7-PC	18.21	436315	56.72
922.78313	56:7 TAG	30.48	427786	57.34
924.80027	56:6 TAG	30.87	426205	57.95
529.40022		3.03	421322	58.56
897.73100		32.11	406721	59.15
803.54379		5.83	406542	59.74
792.55556	40:6-PC	17.02	390699	60.30
848.55850		18.25	389976	60.87
922.78549	56:7 TAG	29.96	381901	61.42
917.70012		30.00	366185	61.95
850.78653	50:1 TAG	32.18	350251	62.46
920.76821	56:8 TAG	28.99	320400	62.92
944.86227	57:3 TAG	31.26	312142	63.37
941.69967		28.99	290513	63.79
917.69868		29.37	282722	64.20
956.86151		30.38	274599	64.60
848.76986	50:2 TAG	31.15	274569	64.99
904.59095		12.68	267470	65.38
734.56824	32:0-PC	18.25	261905	65.76
788.61832	36:1-PC	22.09	261309	66.14
881.75683		32.10	257543	66.51

Compound mass (m/z)	Identification	Retention time	Abundance	Cumulative Abundance %
738.64658		13.40	256428	66.88
815.69480		26.10	252772	67.25
941.69937		29.54	250203	67.61
958.87848	58:3 TAG	31.26	248232	67.97
919.71424		30.29	244829	68.32
946.77996		29.50	241329	68.67
904.83251	54:2 TAG	33.00	227035	69.00
369.35269		32.93	226929	69.33
894.71950		28.49	217631	69.64
569.43321		22.07	201880	69.93
834.75392		31.15	201558	70.22
536.61320		20.61	194946	70.51
627.53518		12.68	191443	70.78
945.72983		30.86	182139	71.05
943.71461		29.95	176429	71.30
919.71527		30.92	175368	71.56
878.81710	52:1 TAG	33.07	166980	71.80
740.52345		14.19	157480	72.03
601.51945		31.25	156482	72.25
775.59333	34:2-PC	15.89	153387	72.47
904.59068		13.13	152651	72.69
391.28472		5.37	151807	72.91
965.69736		28.61	150254	73.13
531.40855		10.91	144512	73.34
804.54889		14.16	144434	73.55
918.75089	56:9 TAG	28.12	144201	73.76
926.81209		31.91	139863	73.96
812.65533		26.38	138741	74.16
577.51691		31.25	138017	74.36
744.55339	36:2 PE	19.14	134981	74.55
647.45947		24.16	131426	74.74
796.57965		16.07	129126	74.93
946.87843	57:2 TAG	32.10	128133	75.12
960.89387	58:2 TAG	32.10	127961	75.30
927.74073		29.95	127427	75.49
575.50331		30.36	126388	75.67
915.68562		29.17	126371	75.85
820.52517		14.06	125109	76.03
819.51692	40:8-PG	5.21	120621	76.21
923.74588		32.22	119736	76.38
888.79936		31.75	118282	76.55
921.73024		31.45	118273	76.72
915.68461		28.49	117066	76.89
627.53495		13.12	115788	77.06

Compound mass (m/z)	Identification	Retention time	Abundance	Cumulative Abundance %
756.55368		13.25	115692	77.23
948.79304		30.71	115116	77.39
832.58344	40:7-PC	13.27	110603	77.55
868.73336		28.82	108377	77.71
813.68365	42:2-SM	23.76	106781	77.86
907.76361		32.03	105764	78.02
869.69988		31.33	104268	78.17
925.72653		29.54	103157	78.32
575.50403		31.26	101786	78.46
577.51948		32.11	99890	78.61
889.66968		28.83	99397	78.75
929.75722		30.86	98625	78.89
867.68365		30.23	97340	79.04
943.71478		30.49	96250	79.17
716.52398	34:2-PE	14.88	96096	79.31
780.55146		14.88	93636	79.45
833.58454		26.38	93542	79.58
796.52968		14.91	93293	79.72
960.76902		20.47	89539	79.85
801.67798		25.09	89163	79.98
822.75414	48:1 TAG	31.20	88909	80.11
844.73775	50:4 TAG	29.25	88661	80.23
970.87694	59:4 TAG	31.20	88176	80.36
750.55772		17.63	87314	80.49
967.71472		29.59	87074	80.61
524.37203	18:0 lyso-PC	4.09	86187	80.74
982.87570	60:6 TAG	30.30	85991	80.86
907.77369	56:6 TAG	32.22	85892	80.99
603.53502		32.10	81053	81.10
856.58189		17.00	80945	81.22
862.78410	52:1 TAG	31.64	79632	81.34
939.68510		28.12	78897	81.45
968.86058	59:5 TAG	30.31	78615	81.56
913.89068		31.15	77328	81.68
927.74499		30.49	75987	81.79
391.28462		5.83	75591	81.90
780.55521	36:5-PC	12.06	75304	82.00
627.53444		18.27	75274	82.11
828.55188		13.15	74020	82.22
836.61552	40:5-PC	20.26	73972	82.33
980.82602		29.37	73510	82.43
623.50359		13.24	73213	82.54
984.89254	60:4 TAG	31.20	72757	82.64
909.73361		31.75	70631	82.75

Compound mass (m/z)	Identification	Retention time	Abundance	Cumulative Abundance %
829.68820		30.70	70094	82.85
980.85947	60:6 TAG	30.00	69370	82.95
1004.79464		19.92	69187	83.05
766.55301		15.69	68351	83.15
948.79995	58:8 TAG	30.42	66419	83.24
966.84450	59:6 TAG	30.00	66379	83.34
569.36451		10.91	66169	83.44
853.72631		31.34	66068	83.53
817.61093		26.38	65706	83.63
570.54783		31.15	61492	83.71
570.54742		11.75	61012	83.80
766.53749		14.33	60888	83.89
553.39010		10.92	60208	83.98
926.81592	56:5 TAG	31.62	59944	84.06
972.89319	59:3 TAG	32.04	59305	84.15
819.51693	40:8-PG	5.88	57673	84.23
824.76978	48:0 TAG	32.25	57494	84.32
969.73044		30.71	57468	84.40
923.74567		32.02	57159	84.48
837.61464		18.25	56472	84.56
820.73836	48:2 TAG	30.27	56397	84.65
680.63316		32.92	55024	84.73
947.74555		31.91	54662	84.80
875.19253		31.25	53732	84.88
948.79651		29.92	53073	84.96
475.41446		22.04	52773	85.04

[1]Compound detection was performed in Progenesis QI (v2.3) using M+H and M+NH4 adducts and default import filtering strength. Peak filtering was set to 2, and identifications were acquired using chemspider search engine using KEGG, LipidMAPS, MassBank, ChemBank, ChEBI and ChEMBL databases with 5ppm precursor tolerance. Identifications were verified with lipidmaps for incorrect adduct detection.

A

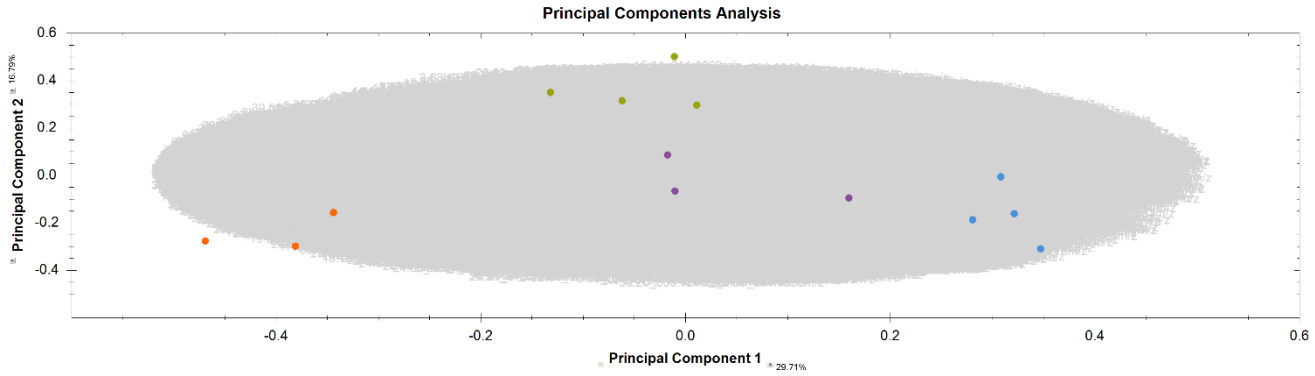

B

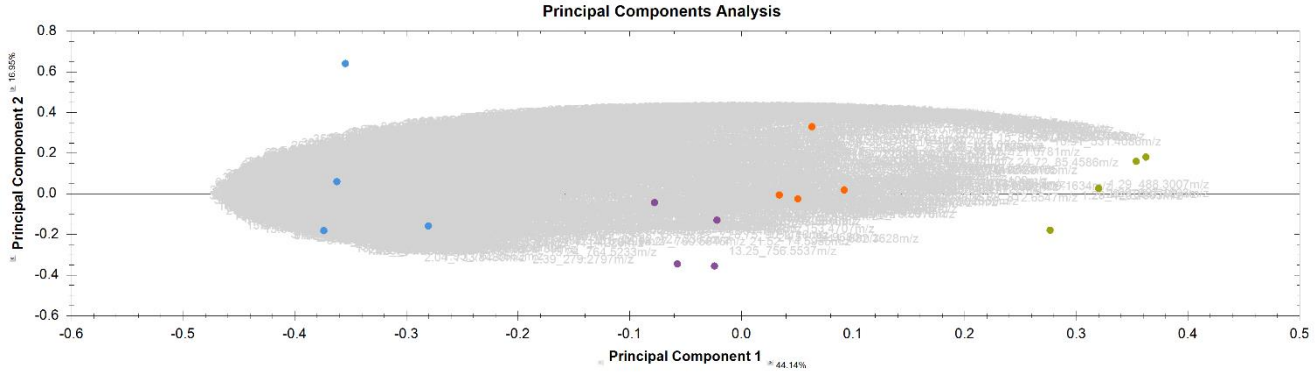

Figure 13. Principal Component Analysis graph for A) Plasma and B) Liver. The distinguishable clustering of each group is indicative of differences being present. The gray cloud is an overlay of the different compounds detected across the samples. Compounds that are closer to a particular cluster is more closely related to it compared to the other.

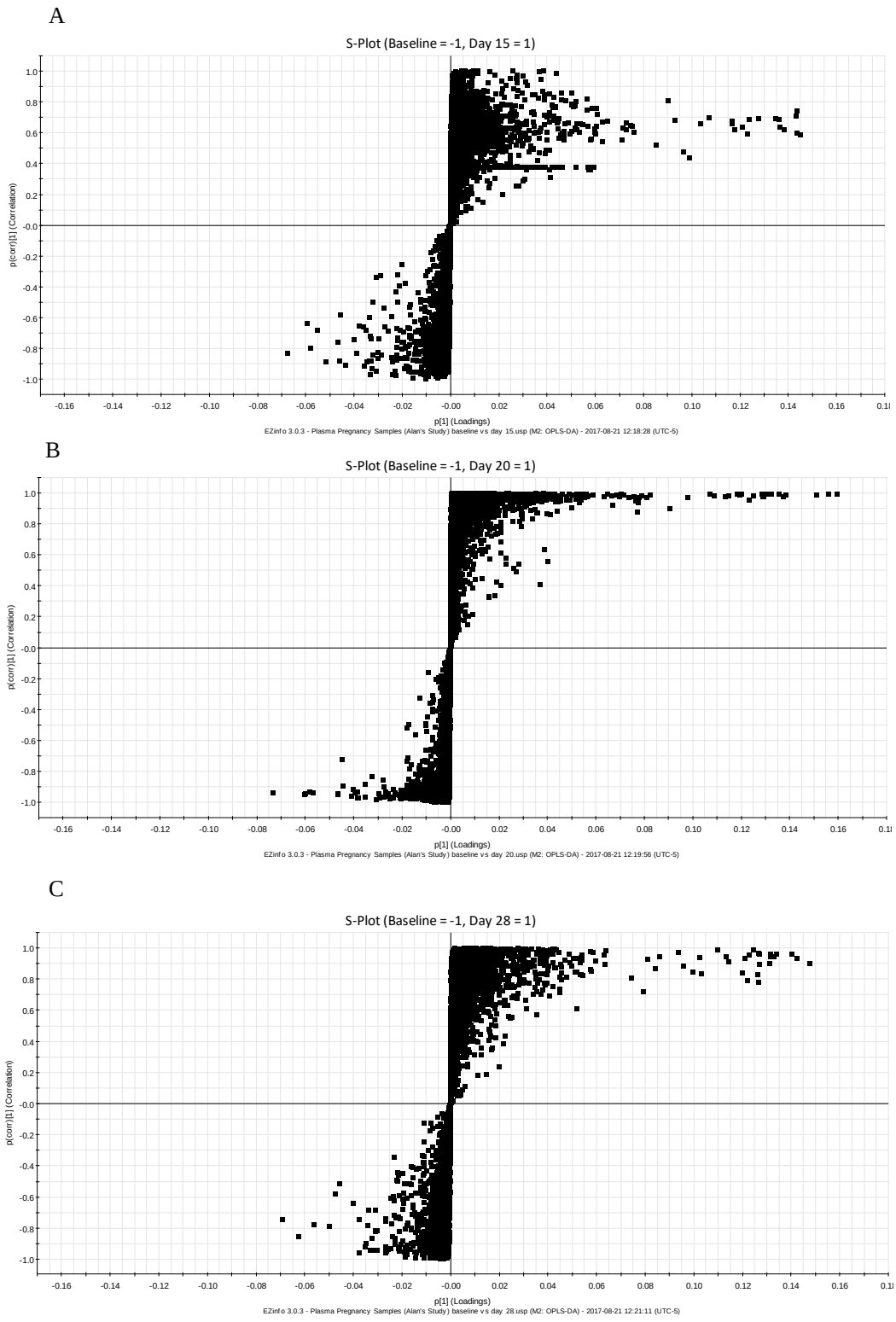

Figure 14. S-plots of plasma samples derived from OPLS-DA. A) Baseline vs. Day 15 B) Baseline vs. Day 20 C) Baseline vs. Day 28. Variables in the upper right part and in the lower left part are up-regulated and down-regulated.

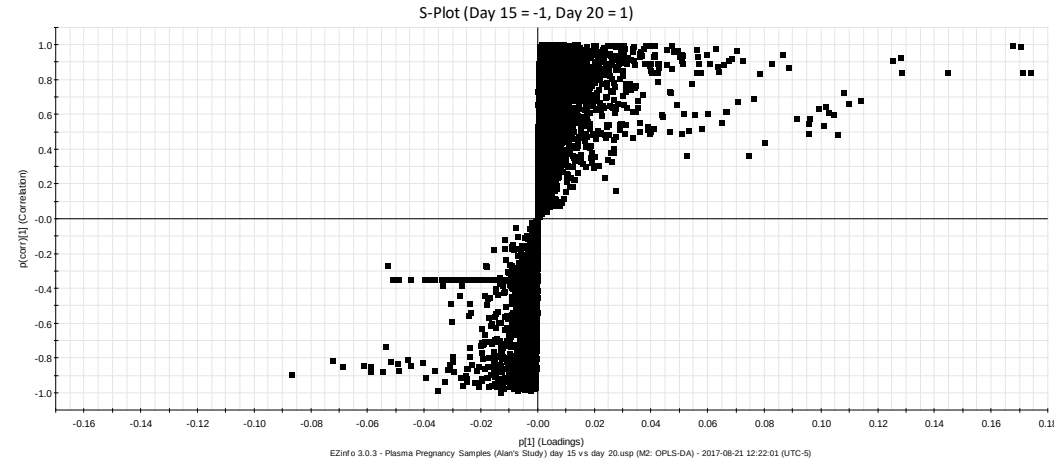

E

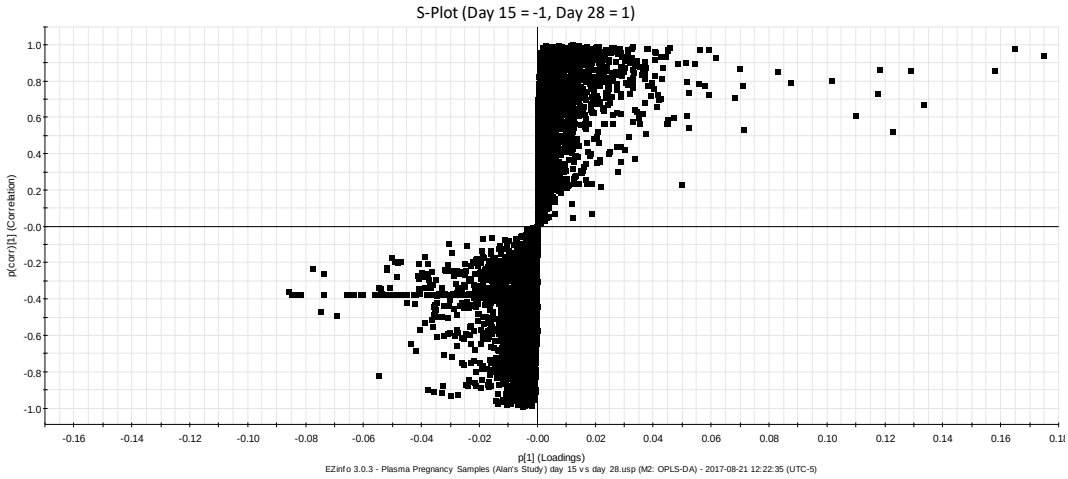

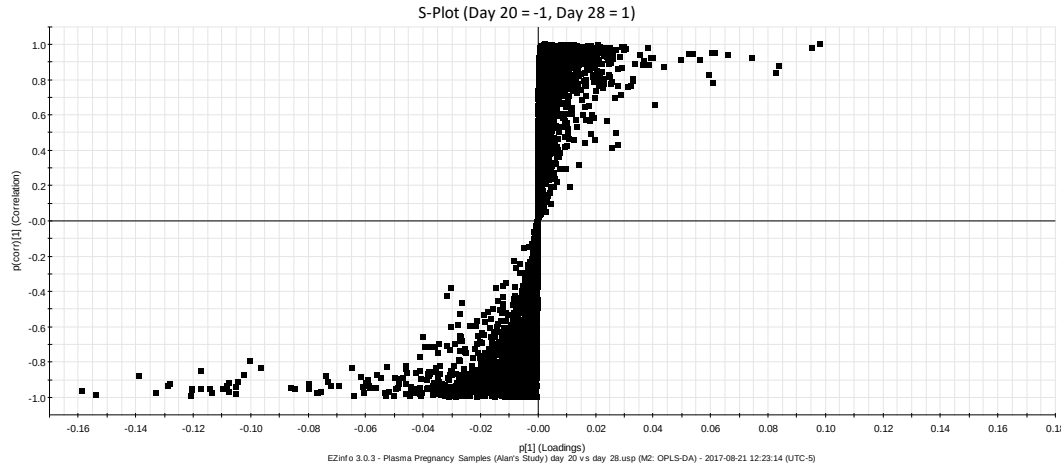

Figure 15. S-plots of plasma samples derived from OPLS-DA. A) Day 15 vs. Day 20 B) Day 15 vs. Day 28 C) Day 20 vs. Day 28. Variables in the upper right part and in the lower left part are up-regulated and down-regulated.

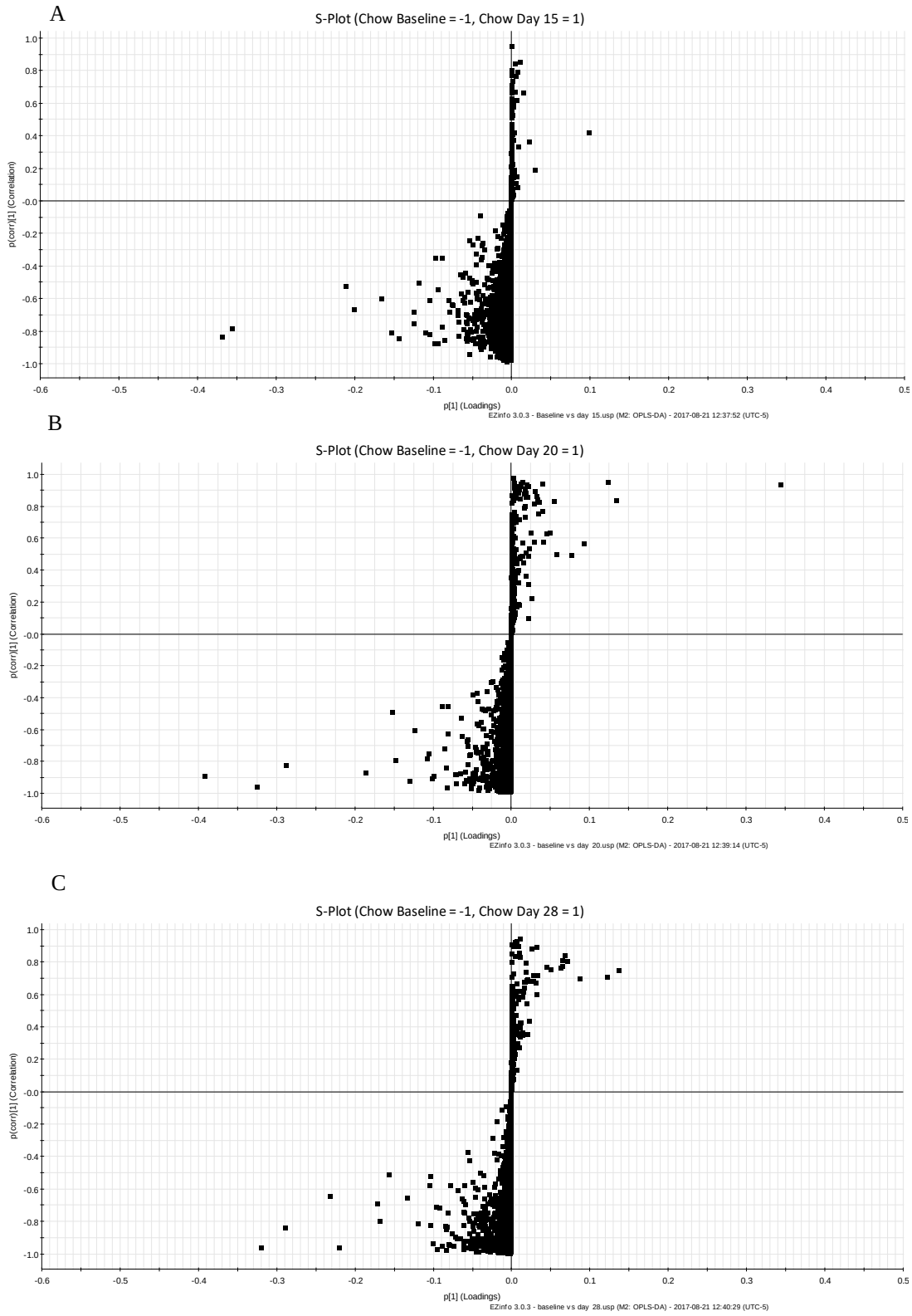

Figure 16. S-plots of liver samples derived from OPLS-DA. A) Baseline vs. Day 15 B) Baseline vs. Day 20 C) Baseline vs. Day 28. Variables in the upper right part and in the lower left part are up-regulated and down-regulated.

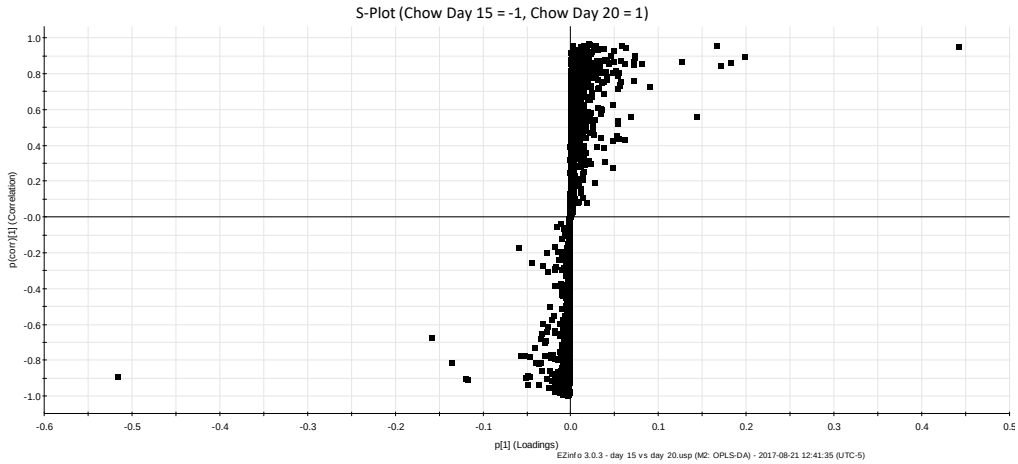

E F

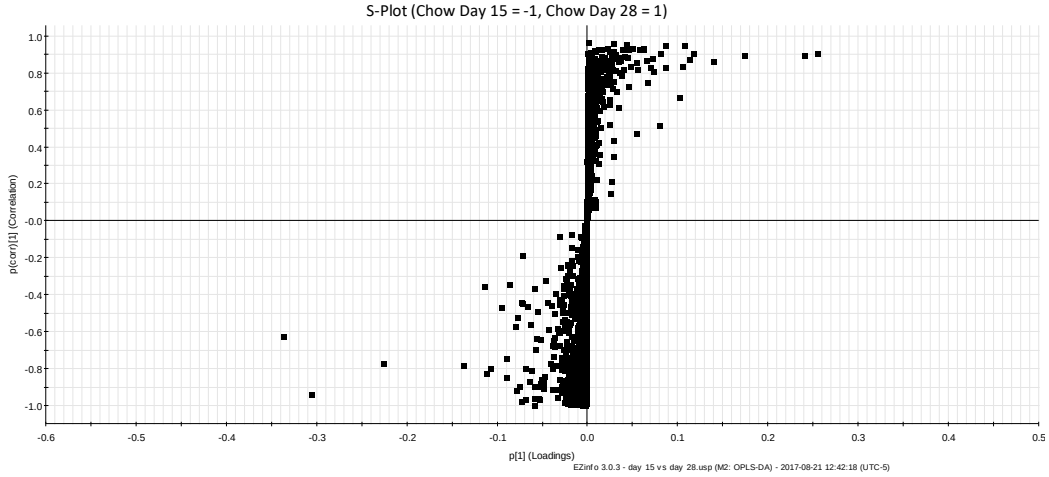

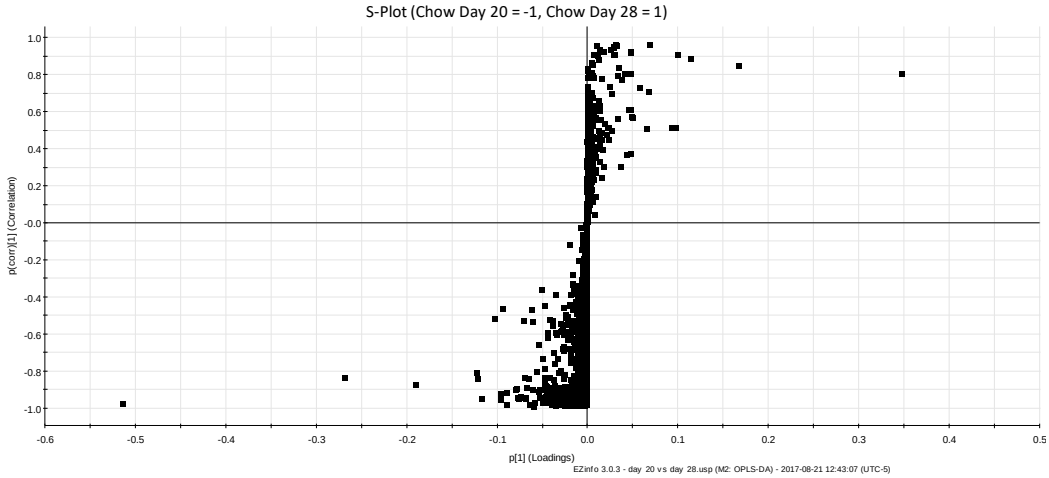

Figure 17. S-plots of liver samples derived from OPLS-DA. A) Day 15 vs. Day 20 B) Day 15 vs. Day 28 C) Day 20 vs. Day 28. Variables in the upper right part and in the lower left part are up-regulated and down-regulated.

Table 4. List of compounds significant in plasma according to s-plot between baseline and day 15. Compounds are ordered based on their fold change.

M/z	Identification	q Value	Max Fold Change	Highest Mean
288.2902		5.23E-04	213.99	Baseline
954.8468	58:5 TAG	0.07	7.71	Day 15
681.4864		0.068	7.40	Day 15
950.8147	58:7 TAG	0.07	6.20	Day 15
994.8787	61:6 TAG	0.067	5.68	Day 15
665.5123		0.077	5.60	Day 15
660.5574	38:5 DAG	0.077	5.32	Day 15
1101.8442		0.207	5.04	Baseline
601.5195		0.079	4.90	Day 15
926.8184	56:5 TAG	0.057	4.63	Day 15
948.8004	58:8 TAG	0.078	4.58	Day 15
671.5760		0.148	4.54	Baseline
972.8024	60:10 TAG	0.078	4.42	Day 15
957.7875		0.068	4.26	Day 15
996.8029	62:12 TAG	0.094	4.15	Day 15
907.7687		0.069	4.03	Day 15
973.7611		0.067	3.98	Day 15
711.5687		0.125	3.93	Baseline
972.8020	60:10 TAG	0.089	3.91	Day 15
931.7725		0.045	3.87	Day 15
947.7447		0.037	3.75	Day 15
924.8056	56:6 TAG	0.082	3.67	Day 15
711.5686		0.115	3.57	Baseline
570.4589		0.002	3.49	Day 15
658.5401	**	0.113	3.39	Day 15
929.7581		0.056	3.39	Day 15
1074.7388		0.014	3.09	Baseline
466.4100		1.26E-04	3.06	Day 15
945.7309		0.041	3.05	Day 15
989.6998		0.032	3.04	Day 15
953.7583		0.082	3.02	Day 15
614.4847		0.01	2.99	Day 15
682.5413		0.095	2.99	Day 15
969.7305		0.077	2.96	Day 15
969.7284		0.059	2.93	Day 15
554.4629		2.94E-04	2.89	Day 15
968.8624	59:5 TAG	0.079	2.88	Day 15
973.7295		0.05	2.87	Day 15
658.5107		0.008	2.86	Day 15
839.6982		0.006	2.84	Baseline
727.5438		0.113	2.82	Baseline
598.4892		2.94E-04	2.82	Day 15
953.7582		0.065	2.82	Day 15
841.7154		0.005	2.71	Baseline
526.4327		0.008	2.70	Day 15
642.5127		0.003	2.60	Day 15
923.7461		0.067	2.59	Day 15
550.3881	20:1 lyso-PC	0.024	2.48	Baseline
907.7726		0.076	2.45	Day 15

M/z	Identification	q Value	Max Fold Change	Highest Mean
709.5894		0.100	2.44	Baseline
730.5645		0.015	2.43	Day 15
725.5633		0.122	2.41	Baseline
672.5258		0.095	2.38	Day 15
905.7574		0.08	2.37	Day 15
628.5003		0.082	2.36	Day 15
921.7307		0.071	2.35	Day 15
702.5363	34:1 PnE	0.02	2.29	Day 15
1063.665		0.037	2.27	Baseline
552.4035	20:0 Lyso-PC	0.041	2.21	Baseline
927.7437		0.078	2.21	Day 15
480.3462	O-16:1 or P-16:0 Lyso-PC	0.056	2.18	Baseline
943.7158		0.059	2.17	Day 15
538.4233	O-20 Lyso-PC	0.067	2.16	Baseline
584.473		0.089	2.14	Day 15
808.5858	38:5-PC	0.096	2.11	Day 15
482.4051		0.015	2.10	Day 15
510.3943	O-18:0 Lyso-PC	0.068	2.07	Baseline
482.3625	O-16:0 Lyso-PC	0.074	2.06	Baseline

Table 5. List of compounds significant in plasma according to s-plot between baseline and day 20. Compounds are ordered based on their fold change.

M/z	Identification	q Value	Max Fold Change	Highest Mean
1061.6507		0.019	88.48	Baseline
974.8169	60:9 TAG	3.46E-04	65.91	Day 20
1063.665		0.004	58.55	Baseline
764.5226	38:6-PE	2.51E-05	55.51	Day 20
1039.673		0.002	40.66	Baseline
1087.6637		0.004	37.26	Baseline
974.8172	60:9 TAG	2.00E-04	32.43	Day 20
924.8681		3.56E-04	32.08	Day 20
954.8468	58:5 TAG	1.51E-04	32.03	Day 20
681.4864		1.08E-04	29.85	Day 20
693.5584		0.001	28.63	Baseline
792.5546	40:6-PE	1.04E-04	28.57	Day 20
1111.639		0.014	26.27	Baseline
1047.6988		0.025	24.82	Baseline
651.5352		1.65E-04	24.35	Day 20
708.558		1.17E-04	23.41	Day 20
858.5992	42:8-PC	2.12E-04	23.3	Day 20
976.833	60:8 TAG	3.33E-04	22.69	Day 20
830.5689	40:8-PC	9.27E-05	22.05	Day 20
665.5123		5.20E-05	21.44	Day 20
660.5574	38:5 DAG	3.25E-05	21.34	Day 20
996.8019	62:12 TAG	0.002	21.33	Day 20
709.5324		9.12E-04	21.22	Baseline
920.8389		2.67E-05	21.03	Day 20
996.8029	62:12 TAG	6.92E-04	20.25	Day 20
944.7734	58:10 TAG	1.43E-04	19.54	Day 20
950.8181	58:7 TAG	1.50E-04	18.69	Day 20
952.8331	58:6 TAG	1.45E-04	18.46	Day 20
946.8548		8.77E-06	18.4	Day 20
625.5195		1.58E-04	18.36	Day 20
337.2745		1.05E-04	18.27	Day 20
994.7859	62:13 TAG	4.08E-04	17.52	Day 20
679.471		5.64E-04	17.19	Day 20
950.8147	58:7 TAG	1.09E-04	16.75	Day 20
994.8787	61:6 TAG	1.86E-04	16.26	Day 20
605.5525		3.11E-04	15.87	Day 20
897.1374		0.001	15.49	Day 20
1015.7151		4.21E-04	14.47	Day 20
623.5041		1.98E-04	14.16	Day 20
808.5903	38:5-PC	2.12E-04	13.83	Day 20
958.8787	58:3 TAG	0.003	13.66	Day 20
972.8024	60:10 TAG	4.29E-04	13.57	Day 20
972.8023	60:10 TAG	9.65E-04	13.22	Day 20
658.5401		1.24E-05	13.1	Day 20
932.8639	56:2 TAG	0.002	12.83	Day 20
972.802	60:10 TAG	4.69E-04	12.78	Day 20
968.7703	60:12 TAG	6.15E-04	12.76	Day 20
926.8184	56:5 TAG	1.02E-04	12.72	Day 20
948.803	58:8 TAG	2.47E-04	12.71	Day 20

M/z	Identification	q Value	Max Fold Change	Highest Mean
930.848		5.30E-04	12.1	Day 20
599.5041		1.38E-04	12.04	Day 20
625.5197		7.00E-04	11.99	Day 20
636.5572		1.19E-04	11.98	Day 20
942.7539		5.85E-04	11.94	Day 20
877.212		6.82E-04	11.84	Day 20
842.7232		3.26E-04	11.63	Day 20
599.5043		1.53E-04	11.57	Day 20
577.5204		2.35E-04	11.56	Day 20
957.7875		8.23E-05	11.44	Day 20
926.8204		2.08E-04	11.42	Day 20
906.8498		0.002	11.41	Day 20
965.6998		3.70E-04	11.4	Day 20
928.8323		1.04E-04	11.28	Day 20
948.8004		2.10E-04	11.25	Day 20
836.6212		5.94E-04	11.22	Day 20
973.7611		7.84E-05	10.9	Day 20
844.7397		2.67E-04	10.86	Day 20
931.7725		8.68E-05	10.82	Day 20
907.7687		1.83E-04	10.68	Day 20
623.5046		1.86E-04	10.52	Day 20
904.8365		2.77E-04	10.49	Day 20
950.8166		1.79E-04	10.44	Day 20
601.519		1.13E-04	10.28	Day 20
603.5389		1.87E-04	10.11	Day 20
947.7447		4.41E-05	10.06	Day 20
878.8217		4.77E-04	10.04	Day 20
949.7287		2.54E-04	9.9	Day 20
634.5413		1.39E-04	9.76	Day 20
570.3577		9.27E-05	9.6	Day 20
994.7855		0.001	9.58	Day 20
655.4704		1.38E-04	9.3	Day 20
864.8028		0.003	9.28	Day 20
866.7221		4.90E-04	9.23	Day 20
992.7703		6.79E-04	9.05	Day 20
639.4965		1.19E-04	8.95	Day 20
725.5633		0.006	8.89	Baseline
602.523		1.15E-04	8.89	Day 20
575.5054		3.21E-04	8.81	Day 20
890.8182		0.001	8.78	Day 20
1013.6995		9.73E-04	8.68	Day 20
575.5042		3.26E-04	8.38	Day 20
909.7557		2.38E-04	8.34	Day 20
577.5244		2.67E-04	8.29	Day 20
657.4863		1.23E-04	8.27	Day 20
709.5894		0.006	8.03	Baseline
682.5413		1.25E-04	8.01	Day 20
924.8056		1.25E-04	7.95	Day 20
947.7467		1.86E-04	7.82	Day 20

M/z	Identification	q Value	Max Fold Change	Highest Mean
768.5547		2.31E-04	7.76	Day 20
931.7732		1.86E-04	7.67	Day 20
997.7252		9.06E-04	7.45	Day 20
844.74		3.82E-04	7.43	Day 20
925.7625		2.10E-04	7.24	Day 20
892.7382		4.43E-04	7.22	Day 20
922.79		2.57E-04	7.11	Day 20
892.7385		6.72E-04	7.02	Day 20
641.5124		1.25E-04	6.92	Day 20
909.789		2.52E-04	6.87	Day 20
902.8211		1.50E-04	6.78	Day 20
897.1844		0.001	6.48	Day 20
850.7894		2.08E-04	6.38	Day 20
894.7542		1.10E-04	6.31	Day 20
860.7712		0.002	6.3	Day 20
888.802		6.28E-04	6.28	Day 20
929.7581		9.67E-05	6.28	Day 20
862.7876		0.002	6.25	Day 20
920.775		1.71E-04	6.16	Day 20
711.5687		0.002	6.09	Baseline
792.5546		3.40E-04	5.96	Day 20
551.5048		4.77E-04	5.74	Day 20
910.7844		2.43E-04	5.69	Day 20
945.7309		6.04E-05	5.67	Day 20
858.7545		0.005	5.65	Day 20
921.731		5.10E-04	5.64	Day 20
946.7896		6.38E-04	5.63	Day 20
899.7107		5.80E-04	5.56	Day 20
905.7575		5.98E-04	5.52	Day 20
915.6843		5.79E-04	5.48	Day 20
903.7418		2.25E-04	5.47	Day 20
882.7542		0.001	5.45	Day 20
894.757		1.38E-04	5.4	Day 20
705.5832		5.62E-04	5.31	Baseline
852.8038		0.002	5.28	Day 20
871.7596		3.23E-04	5.21	Day 20
577.5209		3.01E-04	5.14	Day 20
970.7875		0.002	5.14	Day 20
601.5228		2.31E-04	5.01	Day 20
922.791		1.07E-04	4.97	Day 20
883.7729		3.04E-04	4.93	Day 20
846.7583		5.99E-04	4.89	Day 20
900.8057		1.38E-04	4.85	Day 20
876.8086		3.14E-04	4.78	Day 20
623.504		0.004	4.75	Day 20
920.7722		1.29E-04	4.69	Day 20
898.792		2.92E-04	4.67	Day 20
558.2973		0.002	4.64	Baseline
919.715		3.49E-04	4.62	Day 20

Table 6. List of compounds significant in plasma according to s-plot between baseline and day 28. Compounds are ordered based on their fold change.

M/z	Identification	q Value	Max Fold Change	Highest Mean
619.4822		3.34E-05	859.40	Day 28
1101.8442		0.009	142.67	Baseline
836.9309		0.003	78.27	Day 28
671.576	20:5 CE	0.001	49.39	Baseline
711.5686		0.014	28.86	Baseline
711.5687		0.005	27.82	Baseline
808.9314		0.002	15.55	Day 28
725.526		0.002	15.45	Baseline
899.1526		0.003	14.17	Day 28
709.5521		0.002	13.36	Baseline
901.127		3.49E-04	12.81	Day 28
727.5438		0.002	11.5	Baseline
923.1156		4.63E-04	11.0	Day 28
788.9603		0.008	10.27	Day 28
899.1103		0.001	10.15	Day 28
877.1228		4.16E-04	9.8	Day 28
808.8948		4.81E-04	9.44	Day 28
788.9221		0.002	8.46	Day 28
858.5992	42:8-PC	3.43E-04	8.09	Day 28
897.0947		0.005	7.92	Day 28
877.212		7.32E-04	7.18	Day 28
629.5507		1.91E-04	6.79	Day 28
784.8897		9.25E-04	6.77	Day 28
429.3684		0.001	6.68	Baseline
954.8468	58:5 TAG	0.003	5.86	Day 28
836.6212	40:5-PC	9.02E-04	5.8	Day 28
727.5582		0.009	5.75	Baseline
760.9244		0.006	5.68	Day 28
958.8787	58:3 TAG	0.071	5.42	Day 28
826.5731		0.001	5.29	Day 28
625.5195		0.002	5.06	Day 28
825.7727		6.64E-06	5.05	Day 28
862.6312	40:6-PC	9.16E-05	4.98	Day 28
950.8181	58:7 TAG	7.63E-04	4.96	Day 28
873.0911		0.002	4.86	Day 28
899.2003		0.004	4.86	Day 28
928.8323	56:4 TAG	0.004	4.83	Day 28
603.5389		6.77E-04	4.8	Day 28
783.1465		0.008	4.73	Day 28
932.8639	56:2 TAG	0.03	4.71	Day 28
930.848	56:3 TAG	0.011	4.67	Day 28
808.5903	38:5-PC	9.13E-04	4.62	Day 28
974.8172	60:9 TAG	0.002	4.62	Day 28
780.5542	36:5-PC	0.008	4.54	Day 28
912.8005	55:5 TAG	0.002	4.54	Day 28
890.8182	53:2 TAG	3.11E-04	4.45	Day 28
926.8184	56:5 TAG	6.84E-04	4.45	Day 28
760.8865		3.40E-04	4.42	Day 28
952.8331	58:6 TAG	0.005	4.41	Day 28

M/z	Identification	q Value	Max Fold Change	Highest Mean
808.9784		0.004	4.4	Day 28
888.802		4.63E-04	4.34	Day 28
914.8153		6.35E-04	4.26	Day 28
780.5547		0.015	4.25	Day 28
577.5204		0.005	4.23	Day 28
577.5244		8.63E-04	4.2	Day 28
875.1071		2.40E-04	4.14	Day 28
623.5046		0.006	4.14	Day 28
789.0052		0.004	4.12	Day 28
976.833		0.007	4.11	Day 28
909.7557		4.46E-04	4.06	Day 28
906.8498		0.01	4.04	Day 28
950.8147		0.002	4.04	Day 28
782.9126		0.023	4.02	Day 28
904.8365		0.002	4.01	Day 28
834.9158		0.001	3.99	Day 28
883.2503		6.84E-04	3.99	Baseline
972.8023		0.005	3.92	Day 28
768.5547		1.73E-04	3.88	Day 28
897.1844		0.011	3.88	Day 28
601.519		0.003	3.84	Day 28
602.523		6.14E-04	3.77	Day 28
575.5054		0.014	3.71	Day 28
599.5041		0.006	3.7	Day 28
948.803		0.002	3.68	Day 28
907.7687		6.35E-04	3.68	Day 28
782.8759		0.005	3.67	Day 28
926.8204		0.006	3.63	Day 28
878.8217		0.004	3.61	Day 28
946.8789		6.75E-04	3.6	Day 28
860.7712		5.24E-04	3.59	Day 28
950.8166		0.003	3.58	Day 28
570.4589		2.96E-05	3.55	Day 28
893.7556		5.10E-04	3.54	Day 28
948.8004		0.003	3.49	Day 28
931.7725		5.11E-04	3.48	Day 28
658.5107		6.56E-05	3.46	Day 28
925.7625		0.002	3.45	Day 28
902.8211		8.17E-04	3.35	Day 28
770.5693		0.014	3.34	Day 28
947.7447		2.88E-04	3.33	Day 28
810.9118		0.005	3.33	Day 28
944.7734		0.024	3.32	Day 28
810.9123		0.008	3.32	Day 28
664.6028		0.001	3.31	Day 28
909.789		0.002	3.3	Day 28
432.2389		1.44E-04	3.28	Day 28
957.2692		0.001	3.25	Baseline
1180.3278		0.002	3.23	Baseline

M/z	Identification	q Value	Max Fold Change	Highest Mean
719.5746		0.006	3.21	Baseline
730.5645		1.17E-04	3.19	Day 28
614.4847		7.61E-05	3.18	Day 28
886.7853		8.58E-04	3.17	Day 28
782.6306		0.079	3.16	Day 28
924.8056		9.58E-04	3.15	Day 28
862.7876		4.33E-04	3.15	Day 28
806.8796		3.29E-04	3.14	Day 28
903.7418		0.004	3.14	Day 28
844.7400		0.018	3.13	Day 28
858.7545		0.003	3.1	Day 28
577.5209		0.001	3.1	Day 28
922.7900		0.003	3.09	Day 28
1105.3076		0.001	3.08	Baseline
702.5363		9.17E-05	3.08	Day 28
601.5228		7.91E-04	3.07	Day 28
466.4100		3.10E-05	3.06	Day 28
1031.2884		0.001	3.06	Baseline
947.7467		0.003	3.06	Day 28
919.715		0.003	3.05	Day 28
892.7385		0.041	3.04	Day 28
570.3577		2.30E-04	3.02	Day 28
915.6843		0.006	3.01	Day 28
931.7732		0.004	2.99	Day 28
1047.6988		0.096	2.98	Baseline
735.5486		0.013	2.97	Baseline
876.8086		6.81E-04	2.97	Day 28
598.4892		7.04E-05	2.96	Day 28
884.7675		7.94E-04	2.93	Day 28
1111.639		0.02	2.92	Baseline
554.4629		5.01E-05	2.89	Day 28
929.7581		7.66E-04	2.86	Day 28
910.7844		0.005	2.85	Day 28
899.7107		0.008	2.82	Day 28
445.3664		0.004	2.81	Baseline
642.5127		2.08E-04	2.79	Day 28
725.5633		0.005	2.79	Baseline
746.562		6.55E-05	2.78	Day 28
1091.6983		0.016	2.76	Baseline
945.7309		4.18E-04	2.76	Day 28
972.802		0.009	2.75	Day 28
369.3527		0.001	2.75	Day 28
875.1962		0.002	2.74	Day 28
812.6182		0.001	2.7	Day 28
889.6687		0.044	2.7	Day 28
822.5996		0.006	2.7	Day 28
900.8057		6.85E-04	2.69	Day 28
599.506		0.004	2.69	Day 28
732.5543		0.016	2.66	Day 28

Table 7. List of compounds significant in plasma according to s-plot between day 15 and day 20. Compounds are ordered based on their fold change.

M/z	Identification	q Value	Max Fold Change	Highest Mean
808.6499		0.003	29.63	Day 20
1063.665		0.055	25.84	Day 15
836.6816		0.002	23.94	Day 20
1087.6637		0.057	20.77	Day 15
874.5729		0.059	20.49	Day 20
713.5138		0.057	17.87	Day 20
1039.673		0.04	16.95	Day 15
924.8681		0.031	13.28	Day 20
708.558		0.018	12.33	Day 20
858.5992	42:8-PC	0.044	11.88	Day 20
830.5689	40:8-PC	0.024	11.10	Day 20
709.5324		0.02	10.15	Day 15
1020.8035	64:14 TAG	0.077	9.26	Day 20
974.8169	60:9 TAG	0.07	8.96	Day 20
570.3577	22:5 lyso-PC	0.042	8.12	Day 20
679.471		0.041	7.72	Day 20
946.8548		0.075	6.83	Day 20
808.5903	38:5-PC	0.045	6.79	Day 20
764.5226	38:6-PE	0.095	6.31	Day 20
836.6212	40:5-PC	0.069	6.23	Day 20
792.5546	40:6-PE	0.085	6.19	Day 20
974.8172	60:9 TAG	0.096	6.03	Day 20
994.7859	62:13 TAG	0.076	5.16	Day 20
972.8023	60:10 TAG	0.101	4.89	Day 20
996.8029	62:12 TAG	0.082	4.88	Day 20
1015.7151		0.05	4.83	Day 20
651.5352		0.097	4.71	Day 20
954.8468	58:5 TAG	0.128	4.15	Day 20
965.6998		0.097	4.15	Day 20
944.7734	58:10 TAG	0.156	4.05	Day 20
999.742		0.052	4.05	Day 20
681.4864		0.12	4.03	Day 20
660.5574	38:5 DAG	0.108	4.01	Day 20
976.833	60:8 TAG	0.14	4.00	Day 20
582.2971		0.069	3.95	Day 15
658.5401		0.108	3.86	Day 20
665.5123		0.116	3.83	Day 20
996.8019	62:12 TAG	0.17	3.73	Day 20
949.7287		0.105	3.73	Day 20
337.2745		0.147	3.72	Day 20
544.5997		0.042	3.69	Day 15
807.6372		0.128	3.66	Day 20
625.5197		0.156	3.51	Day 20
558.2973		0.032	3.45	Day 15
994.7855	62:13 TAG	0.142	3.42	Day 20
992.7703	62:14 TAG	0.145	3.29	Day 20
972.802	60:10 TAG	0.112	3.26	Day 20
566.3235		0.056	3.19	Day 15
1013.6995		0.145	3.11	Day 20

M/z	Identification	q Value	Max Fold Change	Highest Mean
952.8331		0.176	3.08	Day 20
968.7703		0.175	3.07	Day 20
972.8024		0.144	3.07	Day 20
625.5195		0.192	3.02	Day 20
997.7252		0.153	2.98	Day 20
942.7539		0.233	2.98	Day 20
544.6646		0.041	2.97	Day 15
663.4955		0.008	2.96	Day 20
520.5968		0.027	2.95	Day 15
950.8181		0.191	2.90	Day 20
994.8787		0.151	2.86	Day 20
1048.182		0.076	2.83	Day 15
931.7725		0.089	2.80	Day 20
926.8184		0.123	2.75	Day 20
973.7611		0.128	2.74	Day 20
623.5041		0.249	2.72	Day 20
950.8147		0.184	2.70	Day 20
958.8787		0.27	2.70	Day 20
682.5413		0.138	2.68	Day 20
947.7447		0.084	2.68	Day 20
957.7875		0.14	2.68	Day 20
907.7687		0.143	2.65	Day 20
791.637		0.024	2.60	Day 15
792.5546		0.132	2.60	Day 20
948.803		0.219	2.59	Day 20
950.8166		0.176	2.51	Day 20
928.8323		0.21	2.47	Day 20
948.8004		0.194	2.46	Day 20
807.1576		0.132	2.44	Day 20
542.3234		0.031	2.39	Day 15
930.848		0.26	2.38	Day 20
520.6578		0.02	2.34	Day 15
524.6265		0.058	2.32	Day 15
599.5041		0.265	2.31	Day 20
838.6339		0.12	2.30	Day 20
806.8796		0.077	2.30	Day 20
577.5204		0.252	2.27	Day 20
946.7896		0.211	2.20	Day 20
970.7875		0.211	2.19	Day 20
924.8056		0.195	2.17	Day 20
623.504		0.266	2.17	Day 20
538.3886		0.089	2.11	Day 15
1041.9351		0.04	2.09	Day 15
806.9645		0.154	2.03	Day 20
1059.7224		0.043	2.02	Day 15
184.0743		0.055	2.01	Day 15
807.3759		0.108	2.01	Day 20
742.5625		0.12	2.01	Day 15

Table 8. List of compounds significant in plasma according to s-plot between day 15 and day 28. Compounds are ordered based on their fold change.

M/z	Identification	q Value	Max Fold Change	Highest Mean
619.4822		0.006	55.74	Day 28
629.5494		0.013	47.05	Day 28
836.9309		0.111	11.82	Day 28
837.0174		0.154	10.94	Day 28
725.526		0.04	9.93	Day 15
709.5521		0.045	8.42	Day 15
812.9249		0.013	8.14	Day 28
629.5507		0.003	7.97	Day 28
808.9314		0.107	5.97	Day 28
808.8948		0.035	4.99	Day 28
788.9603		0.083	4.78	Day 28
788.9221		0.031	4.53	Day 28
653.5498		0.012	4.53	Day 28
784.8897		0.032	4.44	Day 28
832.8984		0.058	4.24	Day 28
952.7485	59:13 TAG	0.034	4.21	Day 15
858.5992	42:8-PC	0.074	4.12	Day 28
727.5582		0.056	4.04	Day 15
816.011		0.054	3.74	Day 28
727.5606		0.058	3.71	Day 15
743.5374		0.062	3.60	Day 15
862.6312	40:6-PC	0.03	3.38	Day 28
813.9951		0.017	3.36	Day 28
826.5731		0.037	3.24	Day 28
836.6212	40:5-PC	0.098	3.22	Day 28
522.6069		0.009	2.91	Day 28
1128.6792		0.006	2.89	Day 28
760.8865		0.021	2.87	Day 28
760.9244		0.175	2.75	Day 28
570.3577		0.12	2.56	Day 28
883.2503		0.009	2.55	Day 15
800.6167	40:2-PE	0.074	2.54	Day 28
786.9079		0.035	2.50	Day 28
664.6028		0.167	2.50	Day 28
789.0052		0.064	2.47	Day 28
603.5353		0.038	2.47	Day 28
812.6182		0.013	2.32	Day 28
808.5903	38:5-PC	0.164	2.27	Day 28
1043.704		0.055	2.23	Day 28
957.2692		0.025	2.23	Day 15
808.9784		0.206	2.22	Day 28
834.9158		0.071	2.22	Day 28
425.1373		0.017	2.19	Day 28
669.5585		0.072	2.18	Day 28
785.5886		0.089	2.14	Day 28
1048.0846		0.16	2.12	Day 28
786.9081		0.052	2.11	Day 28
863.5656		0.037	2.11	Day 28
1031.2884		0.021	2.06	Day 15
1105.3076		0.019	2.01	Day 15

Table 9. List of compounds significant in plasma according to s-plot between day 20 and day 28. Compounds are ordered based on their fold change.

M/z	Identification	q Value	Max Fold Change	Highest Mean
619.4822		0.003	63.96	Day 28
713.5138		0.008	37.77	Day 20
679.471		0.017	29.04	Day 20
808.6499		1.67E-04	22.30	Day 20
924.8681		0.004	17.19	Day 20
708.558		0.003	16.68	Day 20
836.6816		0.001	13.73	Day 20
1020.8035	64:14 TAG	0.006	13.38	Day 20
788.9603		0.002	13.03	Day 28
658.5401		0.013	10.20	Day 20
337.2745		0.016	9.92	Day 20
974.8169	60:9 TAG	0.006	9.65	Day 20
946.8548		0.002	9.61	Day 20
1000.8324	62:10 TAG	0.011	9.14	Day 20
660.5574	38:5 DAG	0.01	9.02	Day 20
920.8389		0.012	8.92	Day 20
681.4864		0.012	8.49	Day 20
665.5123		0.011	8.39	Day 20
807.6372		0.01	8.33	Day 20
922.8519		0.013	8.26	Day 20
792.5546	40:6-PE	0.006	8.23	Day 20
944.8395		0.004	8.05	Day 20
788.9221		0.001	7.93	Day 28
996.8029	62:12 TAG	0.005	7.73	Day 20
974.8172	60:9 TAG	0.006	7.02	Day 20
682.5413		0.011	6.90	Day 20
764.5226	38:6-PE	0.004	6.77	Day 20
994.7859	62:13 TAG	0.003	6.72	Day 20
992.7703	62:14 TAG	0.007	6.36	Day 20
944.7734	58:10 TAG	0.015	5.89	Day 20
651.5352		0.009	5.80	Day 20
996.8019	62:12 TAG	0.018	5.76	Day 20
972.8024	60:10 TAG	0.006	5.59	Day 20
976.833	60:8 TAG	0.011	5.53	Day 20
997.7252		0.007	5.52	Day 20
954.8468	58:5 TAG	0.01	5.47	Day 20
1013.6995		0.008	5.43	Day 20
968.7703	60:12 TAG	0.011	5.35	Day 20
520.5968		0.005	5.20	Day 28
824.6169	42:4-PE	0.015	5.17	Day 28
1015.7151		0.003	5.06	Day 20
830.5689	40:8-PC	0.002	5.05	Day 20
965.6998		0.012	5.02	Day 20
826.5731		0.002	4.78	Day 28
999.742		0.003	4.78	Day 20
994.7855	62:13 TAG	0.012	4.73	Day 20
972.802	60:10 TAG	0.004	4.64	Day 20
603.5353		0.009	4.58	Day 28
949.7287		0.012	4.57	Day 20

M/z	Identification	q Value	Max Fold Change	Highest Mean
812.6182		7.44E-05	4.53	Day 28
623.5041		0.014	4.39	Day 20
952.8331		0.012	4.19	Day 20
942.7539		0.043	4.17	Day 20
950.8147		0.007	4.15	Day 20
599.5043		0.019	4.02	Day 20
824.617		0.011	3.97	Day 28
625.5197		0.004	3.96	Day 20
634.5413		0.046	3.88	Day 20
950.8181		0.007	3.77	Day 20
639.4965		0.044	3.73	Day 20
837.6829		0.011	3.70	Day 28
957.7875		0.006	3.69	Day 20
892.7337		0.01	3.66	Day 20
625.5195		0.011	3.63	Day 20
800.6167		0.014	3.63	Day 28
973.7611		0.006	3.60	Day 20
994.8787		0.006	3.54	Day 20
663.4955		0.004	3.54	Day 20
948.803		0.008	3.46	Day 20
655.4704		0.046	3.45	Day 20
636.5572		0.036	3.44	Day 20
972.8023		0.02	3.37	Day 20
835.6673		0.009	3.33	Day 28
605.5525		0.027	3.32	Day 20
599.5041		0.019	3.25	Day 20
948.8004		0.012	3.23	Day 20
570.3577		4.68E-04	3.18	Day 20
926.8204		0.016	3.15	Day 20
844.7397		0.046	3.12	Day 20
931.7725		0.005	3.11	Day 20
842.7232		0.073	3.10	Day 20
947.7447		0.004	3.02	Day 20
641.5124		0.029	3.00	Day 20
810.9123		0.002	3.00	Day 28
808.5903		0.004	2.99	Day 20
549.4886		0.013	2.95	Day 20
623.504		0.006	2.93	Day 20
950.8166		0.013	2.92	Day 20
907.7687		0.008	2.91	Day 20
792.5546		0.008	2.90	Day 20
184.0742		0.003	2.89	Day 20
858.5992		0.002	2.88	Day 20
657.4863		0.039	2.87	Day 20
926.8184		0.008	2.86	Day 20
878.8217		0.037	2.78	Day 20
538.3886		0.011	2.78	Day 28
850.7894		0.019	2.78	Day 20
892.7382		0.066	2.78	Day 20

M/z	Identification	q Value	Max Fold Change	Highest Mean
920.7750		0.03	2.76	Day 20
577.5204		0.027	2.73	Day 20
800.6169		0.015	2.69	Day 28
601.5190		0.019	2.68	Day 20
866.7221		0.078	2.68	Day 20
551.5048		0.016	2.67	Day 20
542.3234		0.009	2.62	Day 28
904.8365		0.027	2.62	Day 20
599.5038		0.044	2.61	Day 20
930.8480		0.068	2.59	Day 20
575.5042		0.078	2.59	Day 20
842.7216		0.054	2.57	Day 20
953.7582		0.009	2.57	Day 20
931.7732		0.011	2.56	Day 20
573.4888		0.03	2.56	Day 20
947.7467		0.011	2.56	Day 20
970.7875		0.019	2.55	Day 20
905.7575		0.042	2.55	Day 20
623.5046		0.034	2.54	Day 20
921.7310		0.042	2.53	Day 20
820.7405		0.033	2.53	Day 20
924.8056		0.008	2.52	Day 20
968.7711		0.012	2.49	Day 20
946.7896		0.005	2.45	Day 20
808.5858		0.036	2.45	Day 20
894.7542		0.026	2.44	Day 20
1050.7494		0.006	2.43	Day 28
810.9118		0.014	2.39	Day 28
575.5054		0.056	2.37	Day 20
807.1576		0.004	2.37	Day 20
844.74		0.067	2.37	Day 20
848.7727		0.014	2.37	Day 20
602.5230		0.01	2.36	Day 20
871.7596		0.049	2.35	Day 20
928.8323		0.045	2.33	Day 20
846.7583		0.026	2.33	Day 20
892.7385		0.088	2.31	Day 20
922.7900		0.022	2.30	Day 20
807.3759		0.002	2.23	Day 20
787.6727		0.011	2.20	Day 28
929.7581		0.006	2.20	Day 20
824.7709		0.022	2.19	Day 20
806.9645		0.008	2.18	Day 20
920.7722		0.024	2.18	Day 20
801.688		0.007	2.15	Day 28
799.6699		0.017	2.15	Day 28
711.5490		0.020	2.13	Day 28
894.7570		0.053	2.11	Day 20
966.7531		0.025	2.11	Day 20

Table 10. List of compounds significant in liver according to s-plot between baseline and day 15. Compounds are ordered based on their fold change.

M/z	Identification	q Value	Max Fold Change	Highest Mean
875.6118		0.106	7.94	Baseline
873.1752		0.091	7.26	Baseline
873.0917		0.102	6.70	Baseline
873.5927		0.098	6.33	Baseline
946.8784	57:2 TAG	0.057	3.94	Baseline
575.504		0.048	3.91	Baseline
869.6991		0.021	3.65	Baseline
940.8283	57:5 TAG	0.043	3.54	Baseline
601.5195		0.061	3.39	Baseline
960.8939	58:2 TAG	0.05	3.34	Baseline
577.5169		0.03	3.26	Baseline
944.8623	57:3 TAG	0.031	3.17	Baseline
575.5033		0.047	3.16	Baseline
844.7378	50:4 TAG	0.044	3.15	Baseline
549.4899		0.029	3.04	Baseline
865.6673		0.025	3.03	Baseline
874.7883	52:3 TAG	0.049	2.98	Baseline
922.7831	56:7 TAG	0.071	2.92	Baseline
862.7841	51:2 TAG	0.033	2.83	Baseline
867.6837		0.017	2.82	Baseline
920.7671	56:8 TAG	0.061	2.82	Baseline
890.8163	53:2 TAG	0.068	2.80	Baseline
872.7704	52:4 TAG	0.049	2.80	Baseline
820.7384	48:2 TAG	0.049	2.74	Baseline
958.8785	58:3 TAG	0.026	2.72	Baseline
916.8225		0.013	2.69	Baseline
888.7994	53:3 TAG	0.027	2.66	Baseline
956.8615		0.036	2.65	Baseline
1004.854		0.027	2.64	Baseline
883.7155		0.034	2.63	Baseline
930.8415		0.018	2.63	Baseline
881.7568		0.032	2.63	Baseline
954.8264		0.022	2.60	Baseline
990.8433		0.031	2.59	Baseline
914.8108		0.023	2.57	Baseline
1138.791		0.028	2.55	Baseline
932.8539		0.035	2.53	Baseline
889.6697		0.029	2.50	Baseline
822.7541	48:1 TAG	0.038	2.49	Baseline
886.7779		0.025	2.47	Baseline
884.7646		0.027	2.47	Baseline
818.7203	48:3 TAG	0.034	2.46	Baseline
842.7197	50:5 TAG	0.035	2.45	Baseline
631.4698		0.004	2.44	Baseline
920.8593		0.037	2.40	Baseline
925.7265	58:11 TAG	0.033	2.40	Baseline

M/z	Identification	q Value	Max Fold Change	Highest Mean
930.8387		0.021	2.38	Baseline
992.8582		0.025	2.38	Baseline
927.745	58:10 TAG	0.022	2.37	Baseline
897.731		0.029	2.36	Baseline
868.7334		0.05	2.36	Baseline
954.8413		0.027	2.32	Baseline
918.8421		0.028	2.32	Baseline
918.8418		0.024	2.29	Baseline
934.8718		0.025	2.26	Baseline
932.8579		0.023	2.25	Baseline
915.6846		0.081	2.25	Baseline
893.6996		0.035	2.24	Baseline
895.7155		0.022	2.24	Baseline
966.8446	59:6 TAG	0.103	2.23	Baseline
855.7406		0.023	2.21	Baseline
848.7708	58:2 TAG	0.048	2.21	Baseline
909.7336		0.022	2.19	Baseline
941.6994		0.024	2.16	Baseline
948.8000	58:8 TAG	0.069	2.16	Baseline
915.6856		0.074	2.16	Baseline
900.8023		0.116	2.15	Baseline
883.7714		0.081	2.12	Baseline
930.8464	56:3 TAG	0.073	2.12	Baseline
1006.851		0.014	2.10	Baseline
909.7878		0.095	2.08	Baseline
925.7613		0.101	2.08	Baseline
980.8260		0.051	2.08	Baseline
848.7699	50:2 TAG	0.071	2.06	Baseline
952.7673		0.027	2.05	Baseline
972.8932	59:3 TAG	0.067	2.05	Baseline
898.7839	54:5 TAG	0.099	2.04	Baseline
968.8606	59:5 TAG	0.093	2.04	Baseline
982.8757	60:5 TAG	0.089	2.02	Baseline
886.7923		0.037	2.02	Baseline
926.8121		0.098	2.01	Baseline

Table 11. List of compounds significant in liver according to s-plot between baseline and day 20. Compounds are ordered based on their fold change.

M/z	Identification	q Value	Max Fold Change	Highest Mean
810.9098		0.007	Infinity	Baseline
810.9926	18:0/18:1-PC	0.054	354882.18	Baseline
811.3915		0.021	5783.56	Baseline
836.6155	40:5-PC	5.38E-04	6.63	Day 20
575.5033		0.002	4.49	Baseline
575.5040		0.031	3.86	Baseline
716.5240		0.004	3.80	Baseline
601.5195		0.031	3.74	Baseline
848.5585		0.005	3.60	Baseline
794.5681	40:5-PE	0.001	3.58	Day 20
872.7704	52:4 TAG	0.003	3.55	Baseline
744.5534	36:2-PE	0.002	3.34	Baseline
920.7671	56:8 TAG	0.01	3.34	Baseline
844.7378	50:4 TAG	0.017	3.20	Baseline
577.5169		0.013	3.18	Baseline
944.8623	57:3 TAG	0.012	3.13	Baseline
874.7883	52:3 TAG	0.017	3.12	Baseline
796.5297		0.002	3.04	Baseline
889.6697		0.001	3.03	Baseline
806.5695	38:6-PC (16:0/DHA)	0.013	3.01	Day 20
868.7334		9.64E-04	2.93	Baseline
915.6856		0.004	2.93	Baseline
832.5818		0.004	2.90	Baseline
956.8615		0.003	2.83	Baseline
894.7195		0.003	2.79	Baseline
922.7831	56:7 TAG	0.042	2.76	Baseline
944.764		0.027	2.57	Day 20
915.6846		0.01	2.54	Baseline
627.5344		0.001	2.51	Baseline
965.7006		0.016	2.49	Day 20
939.6851		0.005	2.49	Baseline
980.826		0.006	2.46	Baseline
524.372	18:0 Lyso-PC	0.004	2.46	Baseline
925.7265	58:11 TAG	0.006	2.42	Baseline
958.8785	58:3 TAG	0.015	2.42	Baseline
828.5519		0.051	2.26	Day 20
898.7839	54:5 TAG	0.028	2.22	Baseline
768.5546	38:4-PE	0.004	2.21	Baseline
810.6013	38:4-PC	0.008	2.20	Baseline
888.7994	53:3 TAG	0.042	2.18	Baseline
909.7336		0.005	2.12	Baseline
968.8606	59:5 TAG	0.052	2.09	Baseline
844.5263		0.091	2.09	Day 20
918.7509	56:9 TAG	0.003	2.08	Baseline
982.8757	60:6 TAG	0.052	2.01	Baseline

Table 12. List of compounds significant in liver according to s-plot between baseline and day 28. Compounds are ordered based on their fold change.

M/z	Identification	q Value	Max Fold Change	Highest Mean
873.5927		4.19E-06	Infinity	Baseline
875.6118		6.12E-06	Infinity	Baseline
873.0917		7.67E-06	Infinity	Baseline
873.1752		1.30E-05	Infinity	Baseline
810.9098		0.004	Infinity	Baseline
810.9926		0.035	Infinity	Baseline
811.3915		0.006	25901.11	Baseline
875.1925		0.002	1872.77	Baseline
1032.8848		2.85E-04	10.88	Baseline
988.8325	61:9 TAG	3.57E-04	9.26	Baseline
1030.8741		4.47E-04	9.03	Baseline
940.8283	57:5 TAG	6.33E-05	8.30	Baseline
996.8865		4.71E-04	7.11	Baseline
920.7671	56:8 TAG	9.41E-04	7.10	Baseline
990.8433		3.67E-04	6.74	Baseline
966.8446	59:6 TAG	3.57E-04	5.93	Baseline
575.504		0.005	5.92	Baseline
796.5297		1.17E-04	5.83	Baseline
575.5033		5.37E-04	5.79	Baseline
844.7378	50:4 TAG	8.44E-04	5.57	Baseline
973.7243		2.90E-04	5.42	Baseline
601.5195		0.005	5.39	Baseline
922.7831	56:7 TAG	0.005	5.38	Baseline
952.7673		2.50E-04	4.89	Baseline
992.8582		0.001	4.83	Baseline
925.7265	58:11 TAG	3.52E-04	4.74	Baseline
872.556		0.007	4.72	Baseline
954.8264		6.11E-05	4.71	Baseline
850.7865	50:1 TAG	0.025	4.67	Baseline
968.768	60:12 TAG	7.11E-04	4.59	Baseline
844.5263		0.016	4.35	Baseline
989.7009		8.78E-04	4.21	Baseline
549.4899		0.002	4.18	Baseline
842.7197	50:5 TAG	6.24E-04	4.15	Baseline
980.826		2.53E-04	4.08	Baseline
772.5829	35:2-PC	5.38E-04	4.04	Baseline
946.8784	57:2 TAG	0.032	4.02	Baseline
1004.8543		7.30E-04	4.00	Baseline
744.5511	36:2	0.003	3.99	Baseline
968.7506		9.12E-04	3.97	Baseline
948.8000	58:8 TAG	0.002	3.95	Baseline
982.8757	60:6 TAG	7.15E-04	3.86	Baseline
989.7029		0.001	3.84	Baseline
902.8173	54:3 TAG	0.034	3.83	Baseline
968.8606	59:5 TAG	8.07E-04	3.82	Baseline
941.6994		4.88E-04	3.81	Baseline

M/z	Identification	q Value	Max Fold Change	Highest Mean
577.5169		0.004	3.78	Baseline
886.7779		6.13E-04	3.77	Baseline
986.909		0.002	3.70	Baseline
1008.8923		5.03E-04	3.66	Baseline
898.7839		7.30E-04	3.58	Baseline
872.7704		9.15E-04	3.56	Baseline
946.78		3.15E-04	3.55	Baseline
889.6697		9.44E-04	3.49	Baseline
900.8023		0.008	3.46	Baseline
820.5252		0.003	3.43	Baseline
884.7646		3.91E-04	3.43	Baseline
944.8623		0.005	3.43	Baseline
894.7195		4.23E-04	3.41	Baseline
978.8369		1.03E-04	3.41	Baseline
926.8121		0.004	3.37	Baseline
956.8615		6.85E-04	3.36	Baseline
939.6851		3.94E-04	3.34	Baseline
920.7682		6.05E-04	3.31	Baseline
874.7883		0.008	3.30	Baseline
948.7965		3.18E-04	3.27	Baseline
631.4698		2.39E-04	3.27	Baseline
966.8445		3.25E-04	3.27	Baseline
965.6974		3.43E-04	3.26	Baseline
926.8159		0.002	3.25	Baseline
930.8415		0.001	3.25	Baseline
948.793		5.82E-04	3.21	Baseline
915.6846		0.001	3.19	Baseline
927.745		0.001	3.19	Baseline
865.6673		0.002	3.17	Baseline
984.8925		0.002	3.15	Baseline
1138.7913		0.005	3.15	Baseline
909.7336		4.18E-04	3.14	Baseline
927.8165		3.18E-04	3.14	Baseline
974.9088		0.009	3.13	Baseline
930.8464		0.005	3.10	Baseline
980.8595		2.66E-04	3.10	Baseline
924.8003		0.001	3.08	Baseline
868.7334		6.48E-04	3.07	Baseline
836.6155		0.003	3.06	Day 28
828.5519		0.017	3.06	Baseline
731.6041	56:6 TAG	9.23E-04	3.06	Baseline
994.8754		6.24E-04	3.04	Baseline
820.7384		0.006	3.02	Baseline
888.7994		0.004	3.00	Baseline
939.6855		9.41E-04	2.98	Baseline
972.8932		0.004	2.96	Baseline

M/z	Identification	q Value	Max Fold Change	Highest Mean
932.8579		7.82E-04	2.93	Baseline
1006.8507		9.00E-04	2.92	Baseline
972.7992		9.39E-04	2.91	Baseline
960.8939		0.041	2.91	Baseline
950.8124		0.002	2.88	Baseline
970.8769		0.002	2.87	Baseline
922.7855		9.17E-04	2.87	Baseline
934.8718		0.002	2.86	Baseline
1006.8757		3.36E-04	2.85	Baseline
992.861		3.37E-04	2.84	Baseline
862.7841		0.014	2.83	Baseline
890.8163		0.042	2.82	Baseline
968.8603		0.002	2.77	Baseline
932.8539		0.008	2.76	Baseline
954.8413		2.66E-04	2.75	Baseline
970.7819		0.002	2.75	Baseline
941.6997		7.27E-04	2.72	Baseline
918.7509		1.40E-04	2.70	Baseline
982.876		0.001	2.70	Baseline
920.8593		0.007	2.69	Baseline
724.5246		3.15E-04	2.63	Baseline
964.8229		4.52E-04	2.61	Baseline
918.8421		9.06E-04	2.61	Baseline
972.7967		0.001	2.60	Baseline
958.8785		0.006	2.59	Baseline
917.6987		0.005	2.59	Baseline
551.382		4.19E-04	2.58	Baseline
949.7266		2.91E-04	2.57	Baseline
822.7541		0.012	2.56	Baseline
914.8108		5.54E-04	2.52	Baseline
915.6856		0.002	2.50	Baseline
925.7613		0.027	2.47	Baseline
848.5585		0.015	2.46	Baseline
929.7572		7.27E-04	2.45	Baseline
951.7408		3.04E-04	2.45	Baseline
901.6134		0.002	2.45	Baseline
867.6837		0.012	2.42	Baseline
848.7708		0.004	2.42	Baseline
963.6878		3.91E-04	2.42	Baseline
909.7878		0.028	2.42	Baseline
930.8387		0.003	2.39	Baseline
939.8111		0.002	2.39	Baseline
927.7407		8.60E-04	2.36	Baseline
991.7171		0.002	2.36	Baseline
947.7456		9.06E-04	2.31	Baseline
830.5699		4.99E-04	2.28	Baseline

M/z	Identification	q Value	Max Fold Change	Highest Mean
886.7923		8.10E-04	2.27	Baseline
916.8225		0.003	2.27	Baseline
943.7148		0.013	2.25	Baseline
883.7714		0.036	2.25	Baseline
855.7406		0.004	2.24	Baseline
798.544		0.022	2.23	Baseline
734.5682		0.002	2.21	Baseline
953.7617		5.40E-04	2.20	Baseline
856.5819		0.019	2.19	Baseline
1020.7774		0.023	2.15	Baseline
947.7444		0.001	2.13	Baseline
907.7636		0.003	2.08	Baseline
881.7568		0.047	2.07	Baseline
907.7737		0.003	2.05	Baseline
973.761		7.15E-04	2.05	Baseline
918.8418		0.02	2.03	Baseline
832.5818		0.013	2.01	Baseline
945.7298		0.003	2.01	Baseline

Table 13. List of compounds significant in liver according to s-plot between day 15 and day 20. Compounds are ordered based on their fold change.

M/z	Identification	q Value	Max Fold Change	Highest Mean
836.6155		0.002	6.29	Day 20
794.5681	40:5-PE	0.002	4.45	Day 20
848.5585		0.015	3.01	Day 15
832.5818		0.016	2.48	Day 15
806.5695	48:6 (16:0/DHA)	0.005	2.46	Day 20
744.5534	36:2-PE	0.078	2.26	Day 15
766.553		0.01	2.18	Day 20
828.5519		0.036	2.14	Day 20
810.6013	38:4-PC	0.028	2.13	Day 15
808.5837	48:5-PC	0.015	2.09	Day 20
844.5263		0.059	2.05	Day 20
967.7147		0.064	1.98	Day 20
429.2408		0.078	1.83	Day 20
768.5546	38:4-PE	0.068	1.83	Day 15
391.2846		0.076	1.82	Day 20
391.2847		0.082	1.81	Day 20
803.5438		0.084	1.78	Day 20
803.544		0.09	1.78	Day 20
945.7298		0.061	1.69	Day 20
848.7699	50:2 TAG	0.047	1.64	Day 20
796.5796		0.041	1.62	Day 15
819.5169	40:8-PG	0.136	1.58	Day 20
531.4086		0.052	1.57	Day 20
919.7153		0.193	1.52	Day 20
536.6132		0.167	1.50	Day 20
569.4332		0.187	1.50	Day 20
943.7146		0.164	1.48	Day 20
834.7539		0.165	1.44	Day 20
786.5998	36:2-PC	0.189	1.43	Day 15
788.6183	36:1-PC	0.144	1.31	Day 15
829.7993		0.189	1.17	Day 20

Table 14. List of compounds significant in liver according to s-plot between day 15 and day 28. Compounds are ordered based on their fold change.

M/z	Identifications	q Value	Max Fold Change	Highest Mean
844.5263		0.004	9.09	Day 20
828.5519		0.002	6.93	Day 20
806.5695	48:6-PC (16:0/DHA)	0.003	5.37	Day 20
965.7006		0.008	4.30	Day 20
948.8000	58:8 TAG	0.002	3.26	Day 20
926.8159	56:5 TAG	0.004	3.16	Day 20
967.7147		0.005	2.90	Day 20
946.7800		0.008	2.88	Day 20
744.5534	36:2-PE	0.002	2.82	Day 28
948.7930		0.001	2.75	Day 20
969.7304		0.001	2.74	Day 20
924.8003	56:6 TAG	0.009	2.57	Day 20
945.7298		0.003	2.32	Day 20
929.7572		0.004	2.28	Day 20
965.6974		0.046	2.20	Day 20
836.6155	40:5-PC	0.044	2.16	Day 20
920.7671	56:8 TAG	0.011	2.13	Day 20
922.7855	56:7 TAG	0.021	2.12	Day 20
808.5837	48:5-PC	0.026	2.04	Day 20

Table 15. List of compounds significant in liver according to s-plot between day 20 and day 28. Compounds are ordered based on their fold change.

M/z	Identifications	q Value	Max Fold Change	Highest Mean
844.5263		0.004	9.09	Day 20
828.5519		0.002	6.93	Day 20
806.5695	48:6-PC (16:0/DHA)	0.003	5.37	Day 20
965.7006		0.008	4.30	Day 20
948.8000	58:8 TAG	0.002	3.26	Day 20
926.8159	56:5 TAG	0.004	3.16	Day 20
967.7147		0.005	2.90	Day 20
946.7800		0.008	2.88	Day 20
744.5534	36:2-PE	0.002	2.82	Day 28
948.7930		0.001	2.75	Day 20
969.7304		0.001	2.74	Day 20
924.8003	56:6 TAG	0.009	2.57	Day 20
945.7298		0.003	2.32	Day 20
929.7572		0.004	2.28	Day 20
965.6974		0.046	2.20	Day 20
836.6155	40:5-PC	0.044	2.16	Day 20
920.7671	56:8 TAG	0.011	2.13	Day 20
922.7855	56:7 TAG	0.021	2.12	Day 20
808.5837	48:5-PC	0.026	2.04	Day 20

5.5 Discussion

The analysis of this data was performed on two levels. The first approach was a targeted approach to identify lipid acyl species that were already examined using a triple quadrupole mass spectrometer at 15 days and 20 days of pregnancy [19]. The second approach was a non-targeted, discovery assessment of the rat lipidome throughout pregnancy. This was an attempt to identify all lipid compounds, but this was truncated at the level of compounds that made up the 85% of the total ion intensity signal (85% most abundant compounds) due to the large number of compounds detected. Principal component analysis combined with as several s-plots were used on the dataset to indicate compounds that changed during pregnancy list in baseline as well to examine differences between each time point. There was also an attempt to match the measured mass-to-charge of compounds to specific lipid identities. All of the mass spectrometry approaches in this thesis relied on data generated using a QTOF mass spectrometer

For the targeted approach, acyl species of PC in plasma and liver and of PE in liver were examined across all four time points (**Figures 11 and 12).** and compared to previous results examining day 15 and 20 of pregnancy. The present analysis confirmed the main previous finding that 16:0/DHA PC increases dramatically while the increase in 18:0/DHA PC is significant but more modest in plasma between 15 and 20 days of pregnancy. This also confirmed the main observations in liver between 15 and 20 days of pregnancy with 16:0/DHA PC increasing but not 16:0/DHA PE, while 38:4 PC and PE decreased. This analysis also shows a modest increase in plasma 16:0/DHA-PC at day 15 compared with baseline but not the liver. More interestingly, there was a clear decrease in 16:0/DHA-PC in the liver in the postpartum period compared with day 20 of pregnancy, to well below baseline levels. Plasma 16:0/DHA-PC did decrease as well following the same trend as the liver however postpartum levels matched that of baseline levels. A Similar trend was also seen with 18:0/DHA-PC which decreased in the postpartum period compared with day 20 in both plasma and liver however plasma postpartum levels remained elevated compared

with baseline. This continued increase of DHA levels in plasma postpartum coupled with decreased hepatic DHA mobilization may indicate other tissues are responsible for postpartum DHA mobilization. Further investigation into postpartum periods is required as mammary tissue could be responsible for this continued DHA demand for offspring transport through breastmilk [68].

Another interesting observation was the decreased levels of liver arachidonate (ARA, 20:4n-6) in 38:4-PC at day 20 of pregnancy compared with baseline. This decrease would result in similar levels of ARA and DHA due to the high abundance of ARA in baseline. This high abundance could be a factor in why ARA does not increase during pregnancy despite its importance for fetal development [69]. It is also likely that carbon chain length selectivity might be a factor in determining ARA levels as 20 and 22 carbon PUFA follow different change patterns during pregnancy [70].

Using the same dataset, we set out to establish a baseline level of the top 85% most abundant compounds in both plasma and liver. Baseline samples were used to limit the number of compounds as pregnancy would cause an increase in various lipids that might not be present during baseline. This was also used as a reference for any changes that would occur during pregnancy and their impact relative to the presence of other more abundant compounds. This approach for top 85% of the UHPLC signal is not novel as a similar approach has been previously conducted by others [71, 72]. Plasma baseline levels for top 85% provided over 802 compounds compared to 158 for the liver. Therefore, I only attempted to identify the compounds with the top 50% abundancy for plasma of which about 1/3 was successfully identified. The most abundant compounds in the liver were identified at a similar identification success rate of 36% but more surprisingly, 10 individual lipids made up over 40% of the total abundance with 18:0/20:4-PC alone contributing almost 12% of the total abundance of lipids in liver. Overall, the liver contained predominantly PC and TAG species, with a few PE and very limited quantities of other lipid pools.

In contrast, the plasma contained similar ion abundances of PC, TAG, lyso-PC, and PE species as well as smaller pool of other lipids.

The principal component analysis graphs (**Figure 13**) clearly showed differences between the different time points in both liver and plasma. Two plasma samples were removed (from day 15 and day 20) due to issues with Progenesis failing to extract peaks successfully with the settings established. Significant compounds identified from s-plots for both plasma and liver show increases predominantly in the TAG and PC pools, which is consistent with previously available data. Most changes were observed between baseline and day 20 (baseline vs. end of pregnancy) as well as day 20 vs. day 28 (end of pregnancy vs. postpartum). In plasma, the highest increase observed was in two isomers of 60:9 TAG, 38:6-PE and 40:6-PE at the end of pregnancy compared with baseline. Although we were unable to verify the acyl chains of these compounds, it is likely that the PE compounds are 16:0/DHA-PE and 18:0/DHA-PE. A number of TAG species decreased at day 28 compared with day 20, most notably 64:14 TAG and 60:9 TAG that was mentioned earlier.

In the liver, the lipidome changes exhibited a much different pattern as many compounds decreased at day 20 compared with baseline with a few exceptions being 40:5-PC, 40:6-PC, and most importantly 38:6-PC (16:0/DHA-PC). The postpartum time point also showed decreases in a number of compounds such as 16:0/DHA-PC, 58:8 TAG and 56:5 TAG, and with only 36:2-PE increasing at this time point. Interestingly liver 16:0/DHA-PE and 18:0/DHA-PE were relatively stable during pregnancy with evidence of a decrease only at postpartum. It appears that in the liver during pregnancy, there are mechanisms involved in maintaining hepatic DHA status while producing 16:0/DHA PC for export as a component of lipoproteins. After pregnancy, it appears that mechanisms maintaining hepatic DHA status stop, despite what we hypothesize is a continued demand for DHA to support maternal lactation.

Overall, despite our initial objective to characterize the lipidome throughout pregnancy, we were unable to identify compounds past the "*Brutto*" level. This was due in part to the nature of MS^E data collection. In MS^E, the matching of MS data with MS/MS data is not precise, but relies on retention time-matching between parent ions from the low-energy scans (MS data) and daughter ins from high-energy collision-induced dissociation scans (MS/MS data). When many compounds are detected at similar retention times, the ability to match MS/MS data (fragmentation spectra) to MS data (parent ions) become severely compromised. Therefore, specific acyl chains composition ("*medio*" species) and the -*sn* position of the acyl chains ("*genio*" species) cannot be identified. Strategies to improve our MS^E approach are discussed in the next chapter as part of the limitations and future directions of this project.

Chapter 6: Discussion and conclusion

6.1 Discussion

In this section, I will address the proposed hypotheses, and examine the limitations of the research completed and propose possible solutions to be considered for future research. I will also attempt to integrate the gene expression results and the lipidomic findings with the existing literature.

Hypothesis 1. There will be an increased expression of LPCAT1 in maternal hepatic tissue relative to baseline to accommodate the incorporation of DHA into lyso-PC.

Hypothesis 2. There will be an increased expression of Acsl 3, to accommodate the increased DHA remodeling through acyltransferases.

Hypothesis 3. There will be a decrease in the expression of PLA2G15 in maternal hepatic tissue relative to baseline to reduce the remodeling of PC newly synthesized by PEMT.

I hypothesized that I would observes various changes during pregnancy that would result in increased availability of DHA for fetal transport. This included hypotheses that an acyltransferase and an acyl-CoA synthase would be increased to biosynthesis more lipids that contain DHA. I also hypothesized that a phospholipase involved in acyl chain remodeling of lipids would be decreased while lipoprotein assembly enzymes would be increased. Finally, I hypothesized that 16:0/DHA-PC in plasma and liver would be lower at baseline and postpartum as compared with time points during pregnancy. Contrary to my initial hypothesis, there was no increased expression of any acyltransferase that could point to increased remodeling and incorporation of DHA to PC. AGPAT2 mRNA decreased at day 20 compared to baseline ($p>0.05$), pointing to decreased lyso-phosphatidic acid to phosphatidic acid conversion. This results in decreased levels of a number of lipids in the liver such as 18:0/18:1-PC, 52:4 TAG, 36:2-PE, 56:8 TAG, 50:4 TAG as well as other lipids that decreased at day 20 compared to baseline which can be found in **Table 11.** Acsl 3 decreased throughout pregnancy refuting my hypothesis, while Acsl

6 increased during pregnancy. As for the phospholipases, there was decreased mRNA expression throughout pregnancy. As hypothesized, the decreased expression was most prevalent in PLA_2G15 with its mRNA and protein decreased significantly at day 15 and 20 of pregnancy and increased significantly in the post-partum. I believe that this enzyme is responsible for remodeling PEMT synthesized 16:0/DHA-PC during non-pregnant state as observed initially by Ridgway and Vance [10]. This protein's downregulation in pregnancy coupled with the decreased Acsl 3 is believed to result in increased DHA presence in PC which in turn will enrich lipoproteins' membrane with DHA for mobilization.

Hypothesis 4. There will be an increased expression of MTTP, ABCA1, as well as SREBP at the end of pregnancy compared to baseline to support increased VLDL assembly.

Lipoprotein assembly proteins show no mRNA increase during pregnancy, opposing our initial hypothesis. A significant increase was observed in MTTP but only occurred in the post-partum. ApoA1 and A2 increased during pregnancy, however A1 decreased in the postpartum while A2 continued to increase. Although there was no increased expression of lipoprotein assembly proteins, increased activity could be responsible for the hyperlipidemia occurring during pregnancy, as explained earlier with ABCA1. ApoA2 is hypothesized to assist the delivery of DHA to both the placenta as well as mammary tissue. Careful consideration is to be given as the rat model is considered ideal for fatty acid synthesis research in comparison to humans, but fails in mimicking the lipoproteins in humans. It is clear however that lipoproteins play a vital role in the delivery of DHA to the fetus throughout the course of pregnancy as well as postpartum and this data provides HDL as a target for research in more suitable models.

Hypothesis 5. Plasma 16:0/DHA-PC at baseline and postpartum will be similar and lower than levels at day 20.

Hypothesis 6. Hepatic 16:0/DHA-PC at baseline and postpartum will be similar and lower than levels at day 20.

Lipidomic analysis of plasma and liver samples was first used to detect the most abundant lipids in the non-pregnant rats (**Table 2 and 3**), which interestingly points that only 5 PC species and 5 TAG species are responsible for over 40% of the lipid abundances in the liver. Plasma samples on the other hand show that each individual lipid species have much lower contributions to the total abundance. The most abundant lipids in plasma were 6 PC species, contributing ~12% of total abundance combined. As hypothesized, plasma and liver 16:0/DHA-PC significantly decreased in the postpartum alongside 18:0/DHA-PC, pointing to secondary mechanism for DHA mobilization during this period.

6.2 Consolidating the Results with the Literature

PC species that contained DHA (16:0 and 18:0) both increased in plasma and liver at day 20 of pregnancy compared to baseline, however 16:0/DHA decreased below baseline levels in the postpartum, confirming our hypothesis, while 18:0/DHA returned to baseline levels. This could be due to the high demand for mobilization of maternal DHA remaining in the postpartum to support lactation, but a downregulation of hepatic support as a result of changed hormone signaling postpartum. It could be possible, the mobilization and synthesis of DHA for the offspring in the postpartum shifts from primarily being hepatic during pregnancy, to being driven by mammary tissue in the postpartum. Further examination of the post-partum period is clearly needed. PC species containing ARA exhibited a different trend in plasma during pregnancy, which should not be entirely surprising. Although ARA is as important for fetal development as DHA [69], the high abundance of ARA in the lipids of plasma and the liver before and during pregnancy indicates that specialized adaptations to mobilize ARA to meet fetal transport are not necessary. In contrast, DHA levels in plasma can be quite variable and largely dependent on dietary intake habits. Therefore, there may have been evolutionary pressure to develop adaptations during pregnancy to ensure a supply of DHA to meet fetal demand. There is previous evidence suggesting an

adaptation to shift PUFA metabolism towards high amounts of 22 carbon PUFA over 20 carbon PUFA during pregnancy [73].

These results together with our previous PEMT study [19] provides a more in-depth understanding of DHA mobilization during pregnancy. DHA enriched PE is converted to PC through PEMT in the non-pregnant state. Increased expression of PEMT in pregnancy results in higher prevalence of 16:0/DHA-PC, however due to the remodeling effect of PLA_2G15, downregulation of this enzyme is crucial. By ensuring the integrity of this PC species, it allows the liver to incorporate it to lipoproteins membranes to be transferred through the plasma to the fetus. These results also regarding the post-partum period in which PEMT is downregulated to baseline levels and PLA_2G15 is upregulated above baseline levels. As DHA continues to be transported to the offspring through breastmilk, possible alterations to these enzymes as well as mammary tissue enzymes could be responsible for meeting offspring DHA demands. This requires a post-partum focused study to understand DHA mobilization.

6.3 Limitations

This thesis has limitations due to study design and analytical techniques. For study design, extrapolating findings from rodent pregnancy models must be done with caution as brain development differs in humans. The brain growth spurt occurs during the early postpartum of the rat whereas this occurs during pregnancy in humans. Specifically the first week postpartum in the rat pup brain development tends to match human fetus brain development in the third trimester [74]. However, the brain continues to develop in both rats and humans well after the brain growth spurt period, and in humans this can be well into adulthood [75]. At 7 days postpartum in this study, plasma DHA remained increased as compared with baseline suggests that there may be postpartum adaptations to mobilized DHA still occurring in our rat model. Examining the postpartum period more thoroughly in the may provide additional insights.

Analytically, we used a targeted gene expression approach. Previously, we had used a transcriptomics approach [19], but, this was difficult to interpret due to numerous changes in mRNA expression during pregnancy in numerous metabolic pathways, which made it difficult to observe subtler changes in fatty acid and lipid metabolism. Therefore, to examine fatty acid and lipid metabolism, we focused on specific gene product targets. Unfortunately, the lack of both mRNA primers as well as protein antibodies for several acyltransferases limited our ability to examine several gene product targets related to DHA mobilization during the pregnancy. Some primers used also did not span the coding DNA sequence for the intended gene which may explain why significant changes were not observed. In While activity assays have been defined for some of the gene products, many have not and it was difficult to perform such assessments within the timeline of this thesis. Future examination of these enzymes and their activity could yield more in depth understanding of lipid synthesis and mobilization during pregnancy.

The novelty of MS^E data approach presented several challenges. Some of these challenges were similar to the previously conducted transcriptomic analysis, as untargeted "-*omic*" approaches have a tendency to highlight gene products or compounds with large fold changes regardless of absolute abundances. For lipidomics, this can be particularly deceiving as changes in trace level compounds can get highlighted over large absolute changes in highly abundant compounds. This is evident when examining 16:0/DHA-PE fold change increase and its abundance to its PC counterpart. Although the PE molecule had a much higher fold change, its abundance was minimal as compared with 16:0/DHA-PC.

The major limitation with lipidomic analyses in this thesis was the difficulty in identifying specific acyl-species in the lipidome. The high complexity of the samples, the large number of compounds present, and their incomplete chromatographic separation meant that we were unable to link MS and MS/MS data precisely to be able to verify compounds we had not observed previously, despite using software designed for MS^E. This is due to MS^E analysis performing

consecutive scanning ions in low and high energy resulting in parent ions and their fragments, respectively. As many compounds are detected at the same retention time due to co-elution, the association of specific fragments and their parent ion is lost. Consequently, we were unable to address an objective of characterizing the lipidome at the acyl species level throughout pregnancy, and were only able to list *Brutto* species for most of the lipidome. The Progenesis software used provided further obstacles. Compounds were often misidentified compounds, or not detected due to the data import/filtering settings used. While trial and error adjustment of import and peak filters helped detect more compounds of interest, I was not able to improve the misidentification of compounds. This trial and error approach to tweaking the software was also limited by the large size of the raw MS^E data files (7-10GB per sample) which took a long time to import and process. While the MS^E approach had utility in screening samples for lipidome changes across many types of lipids, caution is advised when examining and interpreting the individual lipid species generated as it appears the identifications are often crude and lack the verification that is associated with precisely linked MS/MS data collection approaches such as data dependent acquisition (DDA) using an inclusion list for compounds of interest [76].

The improvement of MS^E although difficult, might still be possible due to the availability of different software employing different analysis algorithms. It is also possible that conducting analysis on less complicated samples might improve our analysis method and yield better strategies for future analysis. It may also possible to improve our resolution and separation of individual compounds by improved chromatography and/or by using ion mobility separation techniques. This would possibly lead to better ability to link MS and MS/MS data and therefore increase the identification rate of compounds.

6.4 Conclusion

During pregnancy, there are many interconnected mechanisms responsible for facilitating and supporting fatty acid mobilization. A critical finding in this thesis was that hepatic Phospholipase

A2 G15 was decreased at 20 days of pregnancy which is associated with the large increase in 16:0/DHA-PC in plasma and liver. This supports a previous hypothesis that there are metabolic adaptations during pregnancy to mobilize DHA into 16:0/DHA-PC in the circulation. Specifically, this finding supports the observation that PC synthesis by PEMT is upregulated during pregnancy [9, 19]. The finding of decreased PLA2G15 during pregnancy also coordinates well with an observation t newly synthesized PC from PEMT is rich in DHA but that in the non-pregnant state, DHA is rapidly removed from the new PC through remodeling [10]. Downregulated PLA2G15 during pregnancy would result in less remodeling of new PC synthesized from PEMT and allow for DHA-rich PC to persist and potentially enter the circulation as a component of lipoproteins.

Lipidomic analysis of plasma and liver samples of pregnant rats identified TAG, PC and PE species that are responsible for pregnancy hyperlipidemia and transportation of fatty acids to the fetus and offspring. This is a novel approach due to the lack of non-targeted analysis of pregnancy tissues, however limitations of the MS^E data compromised the ability to fulling characterize the lipidome throughout pregnancy.

An adequate supply DHA to the fetus and infant during the late stages of pregnancy and postpartum is important for optimal brain development. Maternal DHA blood status during pregnancy is also an important predictor for infant health outcomes such as asthma [77]. We have demonstrated evidence of novel maternal adaptations during pregnancy that suggest that synthesis and mobilization DHA during pregnancy is complex and involves several metabolic pathways. Through this research, we were able to identify an enzyme, PLA2G15 that further supports a role for PEMT in mobilizing DHA as 16:0/DHA-PC for fetal transport. In addition, we provide further mechanistic support that 16:0/DHA PC may be an important blood biomarker of maternal DHA status during pregnancy. Further evaluation of this biomarker in pregnant populations, could lead to improved dietary recommendations for DHA intake during pregnancy, but lead to specific blood

level targets to identify women and their future infants that could benefit from targeted supplementation with DHA during pregnancy.

References:

1. Connor, W.E., M. Neuringer, and S. Reisbick, *Essential fatty acids: The importance of n-3 fatty acids in the retina and brain.* Nutrition reviews, 1992. **50**(4): p. 21-29.
2. Singh, M., *Essential fatty acids, DHA and human brain.* Indian J Pediatr, 2005. **72**(3): p. 239-42.
3. Mozaffarian, D. and J.H.Y. Wu, *Omega-3 Fatty Acids and Cardiovascular Disease: Effects on Risk Factors, Molecular Pathways, and Clinical Events.* Journal of the American College of Cardiology, 2011. **58**(20): p. 2047-2067.
4. Salem, N., Jr., et al., *Mechanisms of action of docosahexaenoic acid in the nervous system.* Lipids, 2001. **36**(9): p. 945-59.
5. Greiner, R.S., et al., *Rats with low levels of brain docosahexaenoic acid show impaired performance in olfactory-based and spatial learning tasks.* Lipids, 1999. **34 Suppl**: p. S239-43.
6. Stark, K.D., et al., *Global survey of the omega-3 fatty acids, docosahexaenoic acid and eicosapentaenoic acid in the blood stream of healthy adults.* Prog Lipid Res, 2016. **63**: p. 132-52.
7. Denomme, J., K.D. Stark, and B.J. Holub, *Directly quantitated dietary (n-3) fatty acid intakes of pregnant Canadian women are lower than current dietary recommendations.* J Nutr, 2005. **135**(2): p. 206-11.
8. Otto, S.J., et al., *Changes in the maternal essential fatty acid profile during early pregnancy and the relation of the profile to diet.* The American Journal of Clinical Nutrition, 2001. **73**(2): p. 302-307.
9. Yan, J., et al., *Pregnancy alters choline dynamics: results of a randomized trial using stable isotope methodology in pregnant and nonpregnant women.* Am J Clin Nutr, 2013. **98**(6): p. 1459-67.
10. Ridgway, N.D. and D. Vance, *Specificity of rat hepatic phosphatidylethanolamine N-methyltransferase for molecular species of diacyl phosphatidylethanolamine.* Journal of Biological Chemistry, 1988. **263**(32): p. 16856-16863.
11. Luan, H., et al., *Non-targeted metabolomics and lipidomics LC–MS data from maternal plasma of 180 healthy pregnant women.* GigaScience, 2015. **4**: p. 16.
12. Steenweg-de Graaff, J.C., et al., *Maternal LC-PUFA status during pregnancy and child problem behavior: the Generation R Study.* Pediatr Res, 2015. **77**(3): p. 489-97.
13. Breckenridge, W.C., G. Gombos, and I.G. Morgan, *The lipid composition of adult rat brain synaptosomal plasma membranes.* Biochim Biophys Acta, 1972. **266**(3): p. 695-707.
14. Kim, H.Y., A.A. Spector, and Z.M. Xiong, *A synaptogenic amide N-docosahexaenoylethanolamide promotes hippocampal development.* Prostaglandins Other Lipid Mediat, 2011. **96**(1-4): p. 114-20.
15. Lim, S.-Y., J. Hoshiba, and N. Salem, *An extraordinary degree of structural specificity is required in neural phospholipids for optimal brain function: n-6 docosapentaenoic acid substitution for docosahexaenoic acid leads to a loss in spatial task performance.* Journal of Neurochemistry, 2005. **95**(3): p. 848-857.
16. Sun, G.Y., et al., *Docosahexaenoic acid (DHA): An essential nutrient and a nutraceutical for brain health and diseases.* Prostaglandins Leukot Essent Fatty Acids, 2017.
17. Makrides, M., L.G. Smithers, and R.A. Gibson, *Role of long-chain polyunsaturated fatty acids in neurodevelopment and growth.* Nestle Nutr Workshop Ser Pediatr Program, 2010. **65**: p. 123-33; discussion 133-6.

18. Pynn, C.J., et al., *Specificity and rate of human and mouse liver and plasma phosphatidylcholine synthesis analyzed in vivo.* J Lipid Res, 2011. **52**(2): p. 399-407.
19. Chalil, A., *Evaluation of the Role of Phospholipids in Fatty Acid Delivery to the Fetus During Pregnancy*. 2013, University of Waterloo.
20. Fadeel, B. and D. Xue, *The ins and outs of phospholipid asymmetry in the plasma membrane: roles in health and disease.* Crit Rev Biochem Mol Biol, 2009. **44**(5): p. 264-77.
21. Vance, J.E. and D.E. Vance, *Phospholipid biosynthesis in mammalian cells.* Biochem Cell Biol, 2004. **82**(1): p. 113-28.
22. Vance, D.E., *Phospholipid methylation in mammals: from biochemistry to physiological function.* Biochim Biophys Acta, 2014. **1838**(6): p. 1477-87.
23. Reo, N.V., M. Adinehzadeh, and B.D. Foy, *Kinetic analyses of liver phosphatidylcholine and phosphatidylethanolamine biosynthesis using (13)C NMR spectroscopy.* Biochim Biophys Acta, 2002. **1580**(2-3): p. 171-88.
24. Ridgway, N.D. and D.E. Vance, *Kinetic mechanism of phosphatidylethanolamine N-methyltransferase.* J Biol Chem, 1988. **263**(32): p. 16864-71.
25. Sundler, R. and B. Akesson, *Regulation of phospholipid biosynthesis in isolated rat hepatocytes. Effect of different substrates.* J Biol Chem, 1975. **250**(9): p. 3359-67.
26. Yamashita, A., T. Sugiura, and K. Waku, *Acyltransferases and transacylases involved in fatty acid remodeling of phospholipids and metabolism of bioactive lipids in mammalian cells.* J Biochem, 1997. **122**(1): p. 1-16.
27. Kanfer, J. and E.P. Kennedy, *Metabolism and Function of Bacterial Lipids. Ii. Biosynthesis of Phospholipids in Escherichia Coli.* J Biol Chem, 1964. **239**: p. 1720-6.
28. Lands, W.E., *Metabolism of glycerolipides; a comparison of lecithin and triglyceride synthesis.* J Biol Chem, 1958. **231**(2): p. 883-8.
29. Shindou, H. and T. Shimizu, *Acyl-CoA:lysophospholipid acyltransferases.* J Biol Chem, 2009. **284**(1): p. 1-5.
30. Marszalek, J.R., et al., *Long-chain acyl-CoA synthetase 6 preferentially promotes DHA metabolism.* J Biol Chem, 2005. **280**(11): p. 10817-26.
31. Pelerin, H., et al., *Gene expression of fatty acid transport and binding proteins in the blood-brain barrier and the cerebral cortex of the rat: differences across development and with different DHA brain status.* Prostaglandins Leukot Essent Fatty Acids, 2014. **91**(5): p. 213-20.
32. Uyama, T., et al., *The tumor suppressor gene H-Rev107 functions as a novel Ca2+-independent cytosolic phospholipase A1/2 of the thiol hydrolase type.* J Lipid Res, 2009. **50**(4): p. 685-93.
33. Pan, Y.H., et al., *Crystal Structure of Human Group X Secreted Phospholipase A2 : ELECTROSTATICALLY NEUTRAL INTERFACIAL BINDING SURFACE TARGETS ZWITTERIONIC MEMBRANES.* Journal of Biological Chemistry, 2002. **277**(32): p. 29086-29093.
34. Green, J.T., S.K. Orr, and R.P. Bazinet, *The emerging role of group VI calcium-independent phospholipase A2 in releasing docosahexaenoic acid from brain phospholipids.* Journal of Lipid Research, 2008. **49**(5): p. 939-944.
35. Singer, A.G., et al., *Interfacial kinetic and binding properties of the complete set of human and mouse groups I, II, V, X, and XII secreted phospholipases A2.* J Biol Chem, 2002. **277**(50): p. 48535-49.
36. Leslie, C.C., et al., *Properties and purification of an arachidonoyl-hydrolyzing phospholipase A2 from a macrophage cell line, RAW 264.7.* Biochim Biophys Acta, 1988. **963**(3): p. 476-92.

37. Dennis, E.A., et al., *Phospholipase A2 enzymes: physical structure, biological function, disease implication, chemical inhibition, and therapeutic intervention.* Chem Rev, 2011. **111**(10): p. 6130-85.
38. Sata, T., R.J. Havel, and A.L. Jones, *Characterization of subfractions of triglyceride-rich lipoproteins separated by gel chromatography from blood plasma of normolipemic and hyperlipemic humans.* Journal of Lipid Research, 1972. **13**(6): p. 757-768.
39. Polozova, A. and N. Salem, *Role of Liver and Plasma Lipoproteins in Selective Transport of n-3 Fatty Acids to Tissues: A Comparative Study of 14C-DHA and 3H-Oleic Acid Tracers.* Journal of Molecular Neuroscience, 2007. **33**(1): p. 56-66.
40. Heath, R.B., et al., *Selective partitioning of dietary fatty acids into the VLDL TG pool in the early postprandial period.* Journal of Lipid Research, 2003. **44**(11): p. 2065-2072.
41. Wassall, S.R., et al., *Effects of dietary fish oil on plasma high density lipoprotein. Electron spin resonance and fluorescence polarization studies of lipid ordering and dynamics.* J Biol Chem, 1992. **267**(12): p. 8168-74.
42. Gibbons, G.F., *Assembly and secretion of hepatic very-low-density lipoprotein.* Biochem J, 1990. **268**(1): p. 1-13.
43. de Jong, J.J.B. and J.B. Marsh, *Biosynthesis of plasma lipoproteins by rat liver ribosomes.* Journal of Biological Chemistry, 1968. **243**(1): p. 192-199.
44. Bell, R.M. and R.A. Coleman, *Enzymes of glycerolipid synthesis in eukaryotes.* Annu Rev Biochem, 1980. **49**: p. 459-87.
45. Bennett, A.J., et al., *Hepatic microsomal triglyceride transfer protein messenger RNA concentrations are increased by dietary cholesterol in hamsters.* FEBS Lett, 1996. **394**(3): p. 247-50.
46. Wetterau, J.R., et al., *Absence of microsomal triglyceride transfer protein in individuals with abetalipoproteinemia.* Science, 1992. **258**(5084): p. 999-1001.
47. Bucher, N.L., P. Overath, and F. Lynen, *beta-Hydroxy-beta-methyl-glutaryl coenzyme A reductase, cleavage and condensing enzymes in relation to cholesterol formation in rat liver.* Biochim Biophys Acta, 1960. **40**: p. 491-501.
48. Wang, S.L., et al., *Coordinate regulation of lipogenesis, the assembly and secretion of apolipoprotein B-containing lipoproteins by sterol response element binding protein 1.* J Biol Chem, 1997. **272**(31): p. 19351-8.
49. Oram, J.F. and J.W. Heinecke, *ATP-binding cassette transporter A1: a cell cholesterol exporter that protects against cardiovascular disease.* Physiol Rev, 2005. **85**(4): p. 1343-72.
50. Duong, P.T., et al., *Characterization and properties of pre beta-HDL particles formed by ABCA1-mediated cellular lipid efflux to apoA-I.* J Lipid Res, 2008. **49**(5): p. 1006-14.
51. Gibellini, F. and T.K. Smith, *The Kennedy pathway--De novo synthesis of phosphatidylethanolamine and phosphatidylcholine.* IUBMB Life, 2010. **62**(6): p. 414-28.
52. Shimizu, T., *Lipid mediators in health and disease: enzymes and receptors as therapeutic targets for the regulation of immunity and inflammation.* Annu Rev Pharmacol Toxicol, 2009. **49**: p. 123-50.
53. Haggarty, P., *Effect of placental function on fatty acid requirements during pregnancy.* Eur J Clin Nutr, 2004. **58**(12): p. 1559-1570.
54. Haggarty, P., *Fatty acid supply to the human fetus.* Annual review of nutrition, 2010. **30**: p. 237-255.
55. Medicine, I.o., *Dietary Reference Intakes for Energy, Carbohydrate, Fiber, Fat, Fatty Acids, Cholesterol, Protein, and Amino Acids*. 2005, Washington, DC: The National Academies Press. 1358.

56. Canada, G.o. *Prenatal Nutrition Guidelines for Health Professionals - Fish and Omega-3 Fatty Acids*. 2009.
57. Koletzko, B., et al., *Dietary fat intakes for pregnant and lactating women.* Br J Nutr, 2007. **98**(5): p. 873-7.
58. Dukic, A., et al., *[Hyperlipidemia and pregnancy]*. Med Pregl, 2009. **62 Suppl 3**: p. 80-4.
59. Burdge, G.C., et al., *Dietary protein restriction of pregnant rats in the F(0) generation induces altered methylation of hepatic gene promoters in the adult male offspring in the F(1) and F(2) generations.* The British journal of nutrition, 2007. **97**(3): p. 435-439.
60. Kitson, A.P., et al., *Tissue-specific sex differences in docosahexaenoic acid and Delta6-desaturase in rats fed a standard chow diet.* Appl Physiol Nutr Metab, 2012. **37**(6): p. 1200-11.
61. Uyama, T., et al., *Characterization of the human tumor suppressors TIG3 and HRASLS2 as phospholipid-metabolizing enzymes.* Biochim Biophys Acta, 2009. **1791**(12): p. 1114-24.
62. Golczak, M., et al., *Structural basis for the acyltransferase activity of lecithin:retinol acyltransferase-like proteins.* J Biol Chem, 2012. **287**(28): p. 23790-807.
63. Lippi, G., et al., *Lipid and lipoprotein profile in physiological pregnancy.* Clin Lab, 2007. **53**(3-4): p. 173-7.
64. Pressler, R. and S. Auvin, *Comparison of Brain Maturation among Species: An Example in Translational Research Suggesting the Possible Use of Bumetanide in Newborn.* Front Neurol, 2013. **4**: p. 36.
65. Folch, J., M. Lees, and G.H. Sloane Stanley, *A simple method for the isolation and purification of total lipides from animal tissues.* J Biol Chem, 1957. **226**(1): p. 497-509.
66. Hancock, S.E., et al., *Decreases in Phospholipids Containing Adrenic and Arachidonic Acids Occur in the Human Hippocampus over the Adult Lifespan.* Lipids, 2015. **50**(9): p. 861-72.
67. Checa, A., C. Bedia, and J. Jaumot, *Lipidomic data analysis: Tutorial, practical guidelines and applications.* Analytica Chimica Acta, 2015. **885**: p. 1-16.
68. Rodriguez-Cruz, M., et al., *Synthesis of long-chain polyunsaturated fatty acids in lactating mammary gland: role of Δ5 and Δ6 desaturases, SREBP-1, PPARα, and PGC-1.* Journal of Lipid Research, 2006. **47**(3): p. 553-560.
69. Hadley, K.B., et al., *The Essentiality of Arachidonic Acid in Infant Development.* Nutrients, 2016. **8**(4): p. 216.
70. Stark, K.D., et al., *Comparison of bloodstream fatty acid composition from African-American women at gestation, delivery, and postpartum.* Journal of Lipid Research, 2005. **46**(3): p. 516-525.
71. Aristizabal Henao, J.J., et al., *Tailored Extraction Procedure Is Required To Ensure Recovery of the Main Lipid Classes in Whole Blood When Profiling the Lipidome of Dried Blood Spots.* Anal Chem, 2016. **88**(19): p. 9391-9396.
72. WC, B. *The Updated Bottom-Up Solution: Using Critical Ratios for Triacylglycerol Structural Analysis by Mass Spectrometry*. in *The 106th Annual American Oil Chemists' Society Meeting*. 2015. Rosen Shingle Creek, Orlando, FL.
73. Stark, K.D., et al., *Comparison of bloodstream fatty acid composition from African-American women at gestation, delivery, and postpartum.* J Lipid Res, 2005. **46**(3): p. 516-25.
74. Clancy, B., et al., *Extrapolating brain development from experimental species to humans.* Neurotoxicology, 2007. **28**(5): p. 931-7.

75. Semple, B.D., et al., *Brain development in rodents and humans: Identifying benchmarks of maturation and vulnerability to injury across species.* Prog Neurobiol, 2013. **106-107**: p. 1-16.
76. Henao, J.J., *Development and Validation of a Human Blood Acyl-Specific Lipidomic Profiling Method for Clinical Applications,* in *Kinesiology*. 2015, University of Waterloo.
77. Bisgaard, H., et al., *Fish Oil-Derived Fatty Acids in Pregnancy and Wheeze and Asthma in Offspring.* N Engl J Med, 2016. **375**(26): p. 2530-9.